



UPPSALA  
UNIVERSITET

UPTEC W 24033

Examensarbete 30 hp

Juni 2024

# Gap-free snow cover mapping in Sweden using satellite observations

---

Oscar Törsleff



## Abstract

Snow cover plays an important part in the global surface energy and water balance. The reflective properties of snow cover results in a high albedo which reflects sunlight and helps keeping the earth cool. Many regions rely on snow melt as a source of drinking water and irrigation for agriculture. With global warming the snow cover dynamics are changing and the demand for accurate snow cover maps is higher than before to better monitor the snow cover and its changes. Especially in high latitude regions such as the Swedish mountain ranges where challenging conditions make snow cover mapping using remote sensing especially difficult. This study aims in the first part to validate the current optical-based snow cover product from Sentinel-2 (FSC<sub>OG</sub>) and microwave-based snow cover product from Interactive Multisensor Snow and Ice Mapping System (IMS) in the mountainous regions of Sweden on ground-based snow depth measurements. The second part aims to improve snow cover mapping by combining the two snow cover products through spatiotemporal fusion which takes advantage of the high temporal resolution of IMS and the high spatial resolution of Sentinel-2 FSC<sub>OG</sub>.

Both snow cover products achieve an accuracy above 90% when validated on in situ SMHI ground station snow cover data, despite much missing data of the Sentinel-2 FSC<sub>OG</sub> product due to cloud and polar nights, and the coarse resolution of the IMS product. The Sentinel-2 FSC<sub>OG</sub> product showed tendencies to underestimate snow cover. The IMS product proved to be better to calculate snow dynamic metrics and overestimated the snow cover instead. A spatiotemporal fusion algorithm was developed which generated a new snow cover product named V2 based on the IMS and Sentinel-2 FSC<sub>OG</sub> product. The V2 product maintained the high spatial resolution of the Sentinel-2 FSC<sub>OG</sub> product while achieving the daily temporal resolution of the IMS product. This newly developed product achieves similar (slightly lower) snow monitoring accuracy as the original products, and significantly limited the effect of cloud cover and polar nights of original the Sentinel-2 FSC<sub>OG</sub> product while retaining its high spatial resolution. This enabled better characterization of snow cover dynamics compared to the Sentinel-2 product but not the IMS product.

The study showed that spatiotemporal fusion of remotely sensed snow cover data can be used for snow cover mapping of mountainous regions in Sweden. By combining snow cover products from multiple sources which includes microwave-based sensors in combination with high spatial resolution optical snow cover products the snow cover can be monitored in greater detail and more frequently than the standalone products. The proposed spatiotemporal algorithm could be used when improved spatial and temporal resolution is prioritized over accuracy.

**Keyword:** Remote sensing, snow cover, validation, spatiotemporal fusion, IMS, Sentinel-2

**Teknisk-naturvetenskapliga fakulteten**

**Uppsala universitet, Uppsala**

Handledare: Jie Zhang Ämnesgranskare: Veijo Pohjola

Examinator: Johan Arnqvist

## Referat

Gap-free snow cover mapping in Sweden using satellite observations

*Oscar Törsleff*

Snötäcket spelar en viktig roll i den globala energi- och vattenbalansen. Snötäcket har högt albedo som reflekterar solljus och hjälper till att hålla nere jordens temperatur. Många områden är beroende av snösmältning som en källa till dricksvatten och bevattning för jordbruk. Med den globala uppvärmningen förändras snötäckets dynamik vilket ökar efterfrågan på exakta snötäckeskartor för att bättre övervaka snötäcket och dess förändringar. Speciellt på högre breddgrader som de svenska fjällregionerna, där utmanande förhållanden gör snötäckeskartering med fjärranalys särskilt svårt. Denna studie syftar i första delen till att validera den nuvarande optiska snötäckeprodukten från Sentinel-2 (FSC<sub>OG</sub>) och mikrovågsbaserade snötäckeprodukten från Interactive Multisensor Snow and Ice Mapping System (IMS). Valideringen utförs i de svenska fjällregionerna mot valideringsdata från markbaserade snödjupsmätningar. Den andra delen syftar till att förbättra snötäckeskarteringen genom att kombinera de två snötäckeprodukterna genom spatiotemporal fusion. Denna metod drar nytta av IMS höga tidsmässiga upplösning och Sentinel-2 FSC<sub>OG</sub>s höga rumsliga upplösning.

Båda snötäckeprodukterna uppnår noggrannhet över 90% när de valideras med SMHI:s markstationsdata. Detta trots ofullständiga data från Sentinel-2 FSC<sub>OG</sub>-produkten på grund av moln och polarnätter, samt IMS-produkternas grova upplösning. Sentinel-2 FSC<sub>OG</sub>-produkten visade tendenser på att underskatta snötäcket. IMS-produkten visade sig vara bättre på att beräkna snötäckets dynamik och överskattade i stället snötäcket. En rumslig och tidsmässig fusionsalgoritm utvecklades som genererade ett nytt dataset kallad V2 baserad på IMS och Sentinel-2 FSC<sub>OG</sub>-dataseten. V2-datasetet bibehöll den höga rumsliga upplösningen från Sentinel-2 FSC<sub>OG</sub>-produkten samtidigt som den uppnådde den dagliga tidsupplösningen från IMS-produkten. Denna nyutvecklade produkt uppnår något lägre snöövervakningsnoggrannhet som de ursprungliga produkterna. Den nyutvecklade snöprodukten begränsade avsevärt effekten av molntäcke och polarnätter i den ursprungliga Sentinel-2 FSC<sub>OG</sub>-produkten samtidigt som dess höga rumsliga upplösning bibehölls. Detta möjliggör bättre kartläggning av snötäckets dynamik jämfört med Sentinel-2 produkten men lägre än IMS produkten.

Studien visade att rumslig och tidsmässig fusion av fjärranalyserade snötäcksdata kan användas för snötäcke-kartläggning i bergsområden i Sverige. Genom att kombinera snötäckeprodukter från flera källor, inklusive mikrovågsbaserade sensorer i kombination med optiska snötäckeprodukter med hög rumslig upplösning, kan snötäcket övervakas mer detaljerat och oftare än med enskilda produkter. Den föreslagna spatiotemporal algoritmen kan användas när förbättrad rumslig och tidsmässig upplösning prioriteras framför noggrannhet.

Nyckelord: Fjärranalys, snötäcke, validering, spatiotemporal fusion, IMS, Sentinel-2

Intuitionen för geovetenskaper; Luft-, vatten- och landskapslära; Naturgeografi  
Geocentrum, Villavägen 16  
752 36 Uppsala

## **Preface**

This master's thesis concludes my studies in Water- and environmental engineering at Uppsala University and the Swedish University of Agricultural Sciences (SLU). The thesis encompasses 30 ECTS credits and was conducted during the spring of 2024. I would like to express my deepest gratitude to my supervisor Jie Zhang, who has supported and guided me throughout this work. I also want to thank Veijo Pohjola, who has acted as the subject reviewer and provided insightful comments. Lastly, I wish to thank Johan Arnqvist for being the examiner for my thesis.

*Oscar Törsleff*  
Uppsala, June 2024

Copyright © Oscar Törsleff and Department of Earth Sciences; Program for Air, Water and Landscape Sciences; Physical Geography

UPTEC W 24 033, ISSN 1401-5765

Digitally published in DiVA, 2024, through Department of Earth Sciences, Uppsala Universitet. (<http://www.diva-portal.org/>)

## POPULÄRVETENSKAPLIG SAMMANFATTNING

Snö spelar en viktig roll i jordens klimat och vattencykel. Snös förmåga att reflektera solljus hjälper att kyla ner ytan på vår planet och är en viktig del i atmosfärens energibalans. Avsmältningen av snötäcket på våren och sommaren förser stora områden med vatten och är en viktig källa till rent dricksvatten för många människor. Det är därför viktigt att kunna förstå och kvantifiera snötäckets utbredning över hela jorden. Att mäta snödjup manuellt på enskilda platser räcker inte till för att förstå hela snötäckets energibalans. Med global uppvärmning är det ännu viktigare att kunna kartlägga snötäckets utbredning och dess påverkan på globala temperaturökningen.

Traditionella metoder för att mäta snötäckets utbredning utnyttjar fjärranalys där satelliter som kan analysera hela jordens används. Att använda optiska bilder från satelliter är en enkel metod för att upptäcka och kartlägga snö med hög rumslig upplösning. Moln och dåliga ljusförhållanden förhindrar ofta satelliterna att ta tillräckligt bra bilder för att kunna särskilja snötäcket. Med satelliter som använder mikrovågsstrålning är det möjligt att upptäcka snö även genom molnen. Eftersom dess bilder täcker en stor area kan de uppnå en hög tidsmässig upplösning till en bekostnad av låg rumslig upplösning.

Sveriges fjällmassiv ligger så pass långt norrut att solens strålar inte räcker till för att mäta snötäcket med optiska bilder under vinterns månader. Detta i kombination med de molntäcken som ofta täcker området skapar utmanande förhållanden för att mäta snötäckets utbredning med hög rumslig och tidsmässig upplösning. Målet med denna studie är därför att undersöka möjligheten att kombinera styrkorna hos två metoder för att kartera snötäcket. Den europeiska satellitkonstellationen Sentinel-2 använder optiska sensorer med hög rumslig upplösning. Interactive Multisensor Snow and Ice Mapping System (IMS) från den amerikanska vädermyndigheten uppnår hög tidsmässig upplösning och baserar sin snötäckesdata flera källor där bland annat bilder från satelliter som använder mikrovågsstrålning.

Studiens första del validerar de två snötäckesprodukterna på referensdata från Svenska Meteorologiska och Hydrologiska Institutionen (SMHI). Båda produkterna visade hög precision med över 90% träffsäkerhet där Sentinel-2 hade en liten fördel. Sentinel-2 tenderade att underestimera snötäcket medan IMS överskattade snötäckets utbredning. Även för estimeringen utav snötäckets säsongsdynamik Sentinel-2 tenderade att överskatta och IMS underskatta det uppmätta snötäcket. IMS fick även värden närmare det sanna värdet från SMHI data jämfört med Sentinel-2.

För att förbättra karteringen av snötäcket togs en algoritm fram. Algoritmen kombinerar den rumsliga upplösningen från Sentinel-2 med den tidsmässiga upplösningen från IMS. En ny snötäckesprodukt för det undersökta området togs fram och fick namnet V2. Den nya produkten bibehåller den höga rumsliga upplösningen från Sentinel-2 med dagliga uppdateringar likt IMS. Metoden minskar påverkan av moln och de otillräckliga ljusförhållanden som ofta råder i de svenska fjällen. Detta ledde till bättre estimering av snötäckets säsongsdynamik med värden bättre än de för Sentinel-2, dock inte lika nära de värden som IMS uppnår. Den totala precisionen var något lägre än de två ursprungliga produkterna.

Studien visade att det är möjligt att kombinera två olika snöprodukter i områden med svåra förhållanden så som svenska fjällen. Kombinationen av hög rumslig och tidsmässig upplösningen från olika snötäckesprodukter ger upphov till en ny produkt där de bästa aspekterna från varje enskild produkt utnyttjas. Metoden är en förbättring mot tidigare de ursprungliga produkterna på vissa parametrar och belyser problemen med moln och otillräckliga ljusförhållanden som normalt är problematiska. Bättre snötäckeskartor kan förbättra hur vi hanterar vattenresurser på ett mer effektivt sätt. Det kan hjälpa samhället att minska risken för översvämningar och vattenbrist. Klimatforskning gynnas av noggrannare snötäckesdata då bättre modeller för energibalansen i atmosfären kan tas fram vilket mer riktiga förutsägelser om global uppvärmning. Genom att integrera den ny algoritmen i befintliga hydrologiska och klimatmodeller kan vi utnyttja naturresurser på ett mer hållbart sätt.

## Table of contents

<b>1</b>	<b>Introduction .....</b>	<b>3</b>
1.1	Purpose .....	4
1.2	Snow Characterization.....	5
1.2.1	Snow Depth/Snow Water Equivalent .....	5
1.2.2	Snow Cover Extent.....	5
1.2.3	Fractional Snow Cover .....	5
1.2.4	Snow cover duration.....	6
1.2.5	Snow cover onset and end date.....	6
1.3	Remote sensing based snow cover mapping .....	6
1.3.1	Normalized Difference Snow Index .....	8
1.4	Spatiotemporal Fusion.....	8
<b>2</b>	<b>Study Area .....</b>	<b>11</b>
<b>3</b>	<b>Data.....</b>	<b>13</b>
3.1	Sentinel-2 FSC <sub>OG</sub> .....	13
3.2	IMS 1km.....	15
3.3	SMHI .....	18
<b>4</b>	<b>Method.....</b>	<b>20</b>
4.1	Validation Sentinel-2 and IMS snow cover products .....	20
4.1.1	Station data extraction for validation.....	20
4.1.2	Statistical metrics for station based validation .....	20
4.2	Cloud impact analysis of Sentinel-2 snow cover product .....	22
4.3	Snow cover dynamics.....	23
4.3.1	Snow cover onset and end date.....	23
4.3.2	Snow cover duration.....	24
4.4	Sentinel-2 and IMS Spatiotemporal fusion algorithm.....	24
4.5	Validation of new V2 dataset and comparison to Sentinel-2 FSC <sub>OG</sub> .....	27
<b>5</b>	<b>Results.....</b>	<b>28</b>
5.1	Point based validation of Sentinel-2 and IMS snow cover products.....	28
5.2	Cloud impact analysis of Sentinel-2 FSC <sub>og</sub> snow cover product.....	30
5.3	Snow cover dynamics from sentinel-2 and IMS snow cover products .....	31
5.4	Station based Validation of V2 dataset from spatiotemporal fusion algorithm	33
5.5	Data availability of V2 snow cover product.....	35
5.6	Part 2: Snow cover dynamics .....	36

5.7	Part 2: Comparison of V2 snow cover product to original Sentinel-2 FSC <sub>og</sub> and IMS snow cover products .....	38
<b>6</b>	<b>Discussions.....</b>	<b>40</b>
6.1	Part 1: Point based validation of Sentinel-2 and IMs snow cover products ...	40
6.2	Part 1: Cloud impact analysis of Sentinel-2 FSC <sub>og</sub> snow cover product.....	41
6.3	Part 1: Snow cover dynamics of Sentinel-2 FSC <sub>og</sub> and IMS snow cover products .....	42
6.4	Part 2: Point based validation of V2 snow cover product .....	43
6.5	Part 2: Data availability of V2 snow cover product .....	43
6.6	Part 2: Snow cover dynamics of V2 snow cover product.....	44
6.7	Part 2: Comparison of V2 snow cover product to original Sentinel-2 FSC <sub>og</sub> and IMS snow cover products .....	44
<b>7</b>	<b>Conclusions.....</b>	<b>46</b>
<b>8</b>	<b>References.....</b>	<b>47</b>
<b>9</b>	<b>Appendix.....</b>	<b>51</b>
9.1	Individual station snow cover product confusion matrix .....	51
9.1.1	FSC <sub>OG</sub> .....	51
9.1.2	IMS .....	54
9.1.3	V2 .....	56

# 1 INTRODUCTION

Snow cover plays a vital role in the global energy and water cycle. Snow covered ground has a high albedo which reflects sunlight and helps keep the earth cool. With the reflective properties of snow it provides a negative radiative forcing leading to a cooling effect from the snow covered areas of the earth (Flanner et al. 2011). With global warming raising the average temperatures in the atmosphere, snow cover dynamics are changing across the snow-covered areas of the earth. In the Northern Hemisphere the snow cover duration has seen a reduction of 5-6 days per decade based on data from 1967-2018 (Bormann et al. 2018). The loss of snow covered areas due to global warming has led to a decrease of the cryospheric cooling further accelerating the heating of earth's atmosphere (Flanner et al. 2011). Knowing the extent and location of the snow cover on earth's surface is crucial for climate research and understanding temperature changes in the earth's atmosphere.

Snow is an important source of drinking water in various parts of the world. Over half of the world's population rely on water from rivers created by snowmelt (Barnett et al. 2005). In places with high precipitation and cold temperatures the snowpack acts as a water storage and provides usable water throughout the year. Continuous melting of the snow feeds rivers and streams bringing water to civilizations downstream. Regions lacking in water storage capacity along the flow path will suffer the most from these changes as they rely on a continuous supply of water from melting snow (Barnett et al. 2005). The water cycle related to snow cover is therefore of great importance to people's well-being all over the world. Accurate snow maps help forecast the snowmelt and subsequently the flow rates of rivers bringing water to settlements.

Snow cover sees high spatial and temporal variations, especially in mountainous areas due to the complex topography. Transportation of snow by wind causes accumulation zones on leeward slopes (Mott et al. 2018) and different slope aspects effect the ablation properties of snow cover in mountains (Largeron et al. 2020a). The scale of spatial variation can be the small scale of individual slopes where local properties such as topographic shading resulting in wind accumulation cause the variation in snow cover. Larger scales affecting separate watersheds are affected by snow precipitation caused by mountain ranges pushing humid airmasses upward into colder air leading to precipitation, also called orographic precipitation. Temperature gradients across different elevations cause variations in snow cover in mountains with very heterogenous topography (Mott et al. 2018).

Accurate snow cover data are essential for hydrological modeling and water resource management (Dong 2018). As snowmelt is a primary water source for many regions (Barnett et al. 2005), precise information on snow cover extent and dynamics is needed to predict water availability and manage reservoirs effectively. Inaccurate snow cover data can lead to poor water management decisions (Andreadis & Lettenmaier 2006), potentially causing water shortages or flooding (Bormann et al. 2018).

Snow cover maps can be generated through ground station measurements, satellite remote sensed observations or airborne observations. Measuring the snow depth on the ground is the easiest way to map the snow cover. This can be done with a measuring stick or automatically with a snow height sensor (Dong 2018). Simple observations of

the ground either by a human at the location or via webcams can give information if snow cover is present or not (Largeron et al. 2020b). Measurements are taken at regular intervals at the same location to create continuous datasets of the state of the snow cover. The spatial variability of the measurements can be very coarse depending on the infrastructure put in place to take measurements. It is possible to use interpolation techniques to extend the snow data to areas in-between stations, this is however at a reduced accuracy. This is the main drawback for in situ snow observations especially in mountainous regions with high variability in the snowpack. The reliability and high accuracy of in situ measurements make them good candidates to use as ground truth data for validation of other snow cover products (Dong 2018).

Satellite remotely sensed snow cover observations utilize the properties of snow in the electromagnetic spectrum to differentiate between snow cover from other surfaces. Remote sensed observations can benefit from the possibility to have coverage of the whole earth when certain sensors are used compared to ground based observations that are limited to a small area (Largeron et al. 2020b). A widely used method for detecting snow in the optical part of the electromagnetic spectrum is through the Normalized Difference Snow Index (NDSI) (Hall et al. 2002), this method is however severely limited by cloud cover. Passive microwave is used for its ability to penetrate cloud cover and achieve a higher temporal resolution at the cost of low spatial resolution. Active microwave radar is used at high spatial resolution and can penetrate clouds but is limited to detecting wet snow cover making them only usable during periods when snow is melting. Airborne methods from for example airplanes or drones can use the same sensors as satellites but achieve much higher spatial resolution because of the shorter distance to the observed medium. They are instead limited by small observable regions due to the limited coverage (Largeron et al. 2020b).

The significant spatial and temporal variations of snow cover in mountainous regions present challenges for accurate monitoring and modeling. Current snow cover products often struggle to capture these variations due to limitations in spatial and temporal resolution, especially in high latitudes where polar darkness occurs (Dietz et al. 2012b). High spatial resolution products provide detailed information but are limited by infrequent updates, whereas high temporal resolution products offer frequent updates but lack the detail needed for fine-scale analysis (Dietz et al. 2012a).

## **1.1 PURPOSE**

This project aims to address the gaps in current snow cover mapping methodologies, particularly focusing on the challenges posed by cloud cover and low light conditions in high-latitude areas. The goal is to enhance the accuracy and reliability of snow cover maps, which are crucial for various environmental, agricultural, and water resource management applications.

Purpose of the project:

- Investigate the accuracy of snow cover products in Swedish mountainous regions.
- Investigate the potential of combining microwave and optical remote sensing data to overcome the limitations of traditional snow cover mapping methods and improve the snow cover mapping at high latitudes.

From the stated purpose of the project the following research questions are presented:

- What is the comparative accuracy of microwave-based remote sensing versus optical-based snow cover products at high latitudes?
- How can combining optical and microwave satellite imaging techniques improve the accuracy of snow cover mapping at high-latitude areas?

## **1.2 SNOW CHARACTERIZATION**

Measuring the dynamics of snow cover can be done using different metrics to quantify and describe different aspects of the snow cover on the ground. They provide information about the snow cover and are suitable for studying trends in the Earth's snow cover. Different aspects of the snow cover properties such as extent, depth and water content are described by these metrics.

### **1.2.1 Snow Depth/Snow Water Equivalent**

Snow water equivalent (SWE) is a measurement of how much water is contained within the snowpack in a specific area. It gives the depth of water in the defined area that the snowpack would melt into in liquid form. It is given by a product of the snow depth and the snow density in the snowpack (CGLS 2024b). Measuring SWE from space can be done with passive microwave sensors but coarse spatial resolution makes it unsuitable for the heterogeneous snow packs found in complex mountainous terrain (Bormann et al. 2018). Efforts to combine remote sensing data with digital elevation models (DEM), land cover information, in situ measurements and meteorological data using a machine learning approach have brought forward an improved estimation of the snowpack compared to using only microwave data (Zhang et al. 2021). SWE provides valuable information for applications interested in the water provided by a melting snowpack. These can be flood forecasting, water level control for hydropower and irrigation in agriculture.

### **1.2.2 Snow Cover Extent**

Snow cover extent (SCE) measures the spatial area covered by snow. It's represented by a binary map of either snow covered ground or non-snow covered ground (Largeron et al. 2020a). The highly dynamic aspects of SCE due to its sensitivity to temperature changes and precipitation makes it an important parameter for Earth's global surface energy budget. It serves as an input to weather forecast modeling and plays an important role in hydrological runoff modelling and flood forecasting (CGLS 2024a).

### **1.2.3 Fractional Snow Cover**

With SCE being a binary estimate of snow cover in each pixel there is no information given about the variability of snow cover within the pixel. Fractional snow cover (FSC) is given as a fraction of the area covered by snow in a pixel. Estimating the FSC in the pixel gives more information about the amount of snow present in the pixel. This is valuable for hydrological modeling as it gives greater detail of information about the snow cover leading to more accurate model simulations (Salomonson & Appel 2004).

#### **1.2.4 Snow cover duration**

Snow cover duration (SCD) refers to the duration that an area is covered by snow over a period. It's an important metric for regions experiencing seasonal snow cover. SCD varies significantly depending on geographical location and are strongly related to latitude and elevation (Dietz et al. 2012b). It is also driven by large weather patterns with higher temperatures and reduced snowfall during winter in recent years leading to decreased SCD. Precipitation in the form of rain instead of snow as a result of increased temperatures is also a factor for decreasing snow cover in the winter (Klein et al. 2016).

#### **1.2.5 Snow cover onset and end date**

Snow cover onset date (SCOD) and snow cover end date (SCED) describes the start of the snow cover season and the end of the snow cover season for a location. In the northern hemisphere the first day of the snow season occurs in the beginning of the fall and the last day occurs in late spring. SCOD and SCED see great spatial variation and the driving factors are latitude and elevation which correlate well with SCOD and SCED in Europe (Dietz et al. 2012b). As climate change increases global temperatures in the atmosphere, later SCOD and earlier SCED are expected to increase even further during the this century (Jylhä et al. 2008).

This study will focus on SCE and FSC for the snow mapping and SCD, SCOD and SCED for the snow cover dynamics for the remote sensed products. The validation data is given in snow depth but can be converted to SCE by using a threshold for the snow depth that should be considered as snow covered ground. These are the metrics used to measure the snow cover and its properties.

### **1.3 REMOTE SENSING BASED SNOW COVER MAPPING**

This section aims to further explain remote sensing to understand the technique behind development of the snow cover products used in this study. Both the snow cover products are explained in greater detail in a later section. One of the snow cover products is purely based on remote sensed optical data. The other product uses a combination of observations for mapping snow cover with microwave based sensors during periods of cloud cover and low light conditions.

Remote sensing is a technology to gather information about earth from a distance. It enables data gathering of the Earth's state and helps make predictions about the future. It gives a global overview and enormous amounts of data for analysis of the planet (Earth Science Data Systems 2024). The basic principle of remote sensing in earth system observations is to measure the emitted radiation from the Earth's surface. All objects emit radiation at different wavelengths, and this enables sensors aboard satellites to measure the different wavelengths emitted by various surfaces. By interpreting the measured radiation and applying physical principles, it is possible to identify and characterize various features of the observed surfaces (Read & Torrado 2009).

A vast variety of satellites are used for remote sensing, studying different parts of the electromagnetic spectrum. Different orbit properties give satellites unique possibilities to facilitate various needs for data acquisition. High geostationary orbits can constantly monitor specific areas, while lower orbits can monitor the whole Earth at cost of less frequent data acquisition for a specific area (Earth Science Data Systems 2024).

Remote sensing provides a significant advantage in some cases over traditional snow data collection methods such as physical in situ measurements. These traditional methods are often limited by accessibility and the geographical scale of the examined area. Remote sensing allows for continuous and extensive coverage of the whole earth (Dong 2018). This is important for highly dynamic environmental variables like snow cover which sees rapid changes and large spatial heterogeneity (Mott et al. 2018).

Remote sensing involves the use of sensors that detect various spectral bands, including visible, infrared, and microwave wavelengths (Largeron et al. 2020b). Each spectral band provides different information about the Earth's surface depending on the interaction between the radiation and the surface. Different surfaces such as vegetation, water and snow cover have different spectral signatures which allows them to be detected using image processing and classification methods. For more detailed spectral analysis, multispectral sensors can be used. These have more spectral bands which allow more details in the electromagnetic spectrum to be studied (Read & Torrado 2009).

The revisit time of a polar orbiting satellite determines the time it takes for a satellite to visit the same location twice, this is known as temporal resolution. High temporal resolution is crucial for monitoring changes in dynamic environmental variables like snow cover, vegetation and natural disaster monitoring. Satellites with frequent revisit times and thus high temporal resolution are well-suited for monitoring these changes (Belgiu & Stein 2019). A satellite can be stationary in the sky offering a fixed view of the earth, this is referred to as geostationary orbits. By orbiting the earth in exactly one day over the equator the satellite stays in the same place in the sky relative to an observer on earth. This allows for continuous monitoring a certain part of earth's surface. This is common for meteorological and communicating satellites. These satellites can achieve temporal resolutions of minutes at a cost of lower resolution at a scale of kilometers (Liang & Wang 2020). The viewing angle of geostationary satellites makes observations at high latitudes unusable since the images of the surface become distorted (Penn State n.d). Spatial resolution refers to the smallest feature that can be detected by a satellite sensor. Essentially it refers to the pixel size in an image obtained from remote sensing, relative to the area it covers on Earth. High spatial resolution sensors can capture fine details and changes over small areas. This is useful for applications where large spatial variability is present such as forestry and snow modelling. However, higher spatial resolution comes at the expense of lower temporal resolution since higher resolution satellites cover a smaller portion of the earth's surface requiring more revolutions to cover the whole earth (Earth Science Data Systems 2024).

The electromagnetic spectrum has several regions used for different remote sensing applications. Sensors onboard satellites are constructed to operate in specific parts of the spectrum. These regions are typically visible, infrared and microwave (Read & Torrado 2009). The Sentinel-2 satellites used in this study operate in the visible to short wave infrared part of the spectrum. Another satellite of the same Sentinel mission, the Sentinel-3 satellite, carry other types of sensors that for example use microwaves instead. A satellite can also, like the Sentinel-3, have active sensors which emit and receive radiation. An example of this is the synthetic aperture radar (SAR) sensor aboard the Sentinel-3 satellite (European Space Agency 2024). The requirement of an application dictates which satellites and sensors that can be used in remote sensing

applications. Therefore it is important to understand the radiometric properties of a material that is to be studied so the right satellite and sensors can be chosen (Read & Torrado 2009).

### **1.3.1 Normalized Difference Snow Index**

To map snow from space using optical images it is essential to distinguish pixels from many other surface categories. Differentiating between snow and cloud is the main concern since they share a similar spectral reflectance in the visible part of the spectrum (Dozier 1989). Analyzing the texture of cloud and snow pixels can be used to distinguish them from each other. The computational complexity of this operation becomes a limit when handling large amounts of data, which is needed to map snow on a global scale. Therefore, this is not feasible (Dozier 1989).

Using multispectral sensors enables differences in other than the visible spectrum to be used. The same reflectance is observed in the visible spectrum for both clouds whilst snow has a lower reflectance in the near-infrared (NIR) spectrum at 1.55 to 1.75  $\mu\text{m}$  (Hall & Riggs 2010). This is due to the larger grain size of snow which is mostly composed of ice particles.

A normalized difference for snow detection was first developed by Dozier (1989) for the Landsat Thematic Mapper to automate mapping of snow. Utilizing the previously described spectral properties of snow and clouds a normalized difference of band 2 (0.52 – 0.60 $\mu\text{m}$ ) and band 5 (1.55 – 1.75 $\mu\text{m}$ ) from the Landsat Thematic mapper could be used to automate the classification of snow in remote sensed images. The term normalized-difference snow index (NDSI) was devised by Riggs et al. (Hall et al. 1995) during development of a new snow detection algorithm for the data from the new moderate resolution imaging spectroradiometer (MODIS). The algorithm used bands with similar wavelengths to what was used by Dozier (1989). These were MODIS band 4 (0.545 – 0.565 $\mu\text{m}$ ) and band 6 (1.628 – 1.652 $\mu\text{m}$ ). The MODIS snow mapping algorithm also took into account the different reflectance due to dense canopy's in forested areas as detected by the Normalized Difference Vegetation Index (NDVI) (Hall & Riggs 2010). The NDSI algorithm is used for other snow cover products and are adapted to the spectral bands of the satellites used. For NDSI with the Sentinel-2 satellite the green (492.4 $\mu\text{m}$ ) and short wave infrared (1373.5 $\mu\text{m}$ ) bands are used (HR-S&I 2023).

Utilizing the NDSI SCE can be estimated using optical images and a threshold applied to the NDSI value. This threshold is typically 0.4 with values above being classified as snow cover (Dozier 1989). FSC is derived in remote sensed optical images as a function of NDSI. NDSI has proven to have a linear relationship with snow cover for the MODIS snow product (Salomonson & Appel 2004). It is utilized as part of the process for determining FSC on the ground for the Sentinel-2 snow cover product by Copernicus land monitoring service (HR-S&I 2023).

## **1.4 SPATIOTEMPORAL FUSION**

Spatiotemporal fusion is a method that aims to integrate multitemporal and multispectral satellite images to produce a high-resolution dataset by combining the best aspects of multiple data sources. The technique can be used to fill in data gaps caused by cloud cover and insufficient illumination as well as improve the temporal resolution in remote sensed data with low temporal resolution. Figure 1 shows how the

combination of two datasets with one of coarse spatial resolution and one with high spatial resolution generate a dataset with both high spatial and temporal resolution. The ultimate goal is to generate a higher more refined product which provide more information to various use cases (Pohl & Van Genderen 1998).

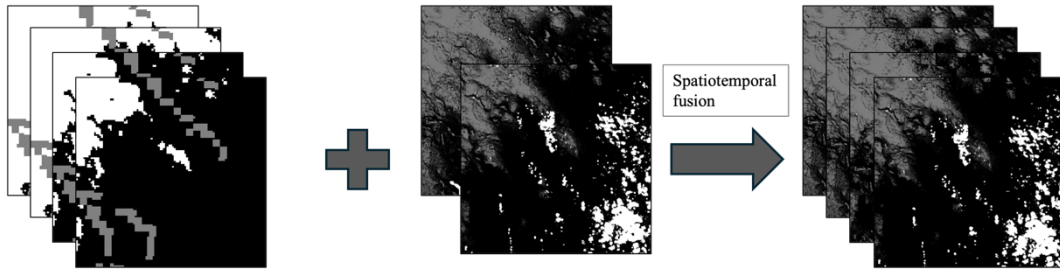


Figure 1: A coarse spatial resolution dataset with high temporal resolution is combined using spatiotemporal fusion with a high spatial but low temporal resolution dataset to create a new dataset with both high spatial and temporal resolution.

An example of sensors which can be combined in spatiotemporal fusion is the very high temporal resolution optical MODIS sensor. The coarse spatial resolution of a couple of hundred meters (Hall et al. 2002) is not sufficient for some applications making it unsuitable where high spatial variability occurs. In contrast higher spatial resolution sensors such as Sentinel-2, providing a spatial resolution of 20m (European Space Agency 2024), can achieve high enough spatial resolution for mapping snow cover. The temporal resolution of 5 days (European Space Agency 2024) is however not enough for all scenarios. A resulting synthesized combined dataset can achieve the high temporal resolution of the MODIS sensor and the high spatial resolution of the Sentinel-2 sensor. This approach facilitates better monitoring of highly dynamic processes at a smaller scales (Zhu et al. 2018).

According to Belgiu and Stein (2019) the challenge of cloud cover causing unusable image data from optical satellites is the biggest use case for spatiotemporal fusion. Combating this issue with spatiotemporal fusion enables the creation of uninterrupted time-series allowing more accurate and consistent monitoring of the environment. Insufficient illumination in high latitudes as a result of polar darkness are described by Dietz et al. (2012b) as a problem for snow cover mapping using the optical MODIS sensor. When not enough light from the sun hits the surface, it is not possible to map the snow cover. At the polar circle at 66°N as much as 71 days are not available in the MODIS snow cover data due to polar darkness. Spatiotemporal fusion can be used to overcome these limitations by using other sensors capable of mapping snow even with the absence of sunlight.

One challenge presented with spatiotemporal fusion is the low computational efficiency which limits the feasibility of implementing these methods effectively in real-world applications. Many current methods require intensive computations for each pixel to fuse the two input datasets to a usable product (Zhu et al. 2018). Zhu et al. (2018) gives an example of using the techniques on one Landsat scene, about 37 million pixels. The computation takes several hours or even days for the one Landsat scene. This limits the use of the methods to small areas or infrequent uses. The use of parallelization, cloud computing and utilization of specified computing hardware suitable for pixelwise operations such as GPUs can mitigate these issues in the future (Zhu et al. 2018).

Esmaeelzadeh et al. (2024) has explored the opportunities presented with fusing Sentinel-2 FSC data with Sentinel-1 wet snow cover maps. The high-resolution Sentinel-2 optical images are limited by cloud cover and polar night. The Sentinel-1 wet snow cover product uses SAR and are thus not hindered by cloud cover. The downside of the Sentinel-1 snow cover product is that it only detects wet snow. Esmaeelzadeh et al. (2024) shows promising results in fusing the two snow cover products to create a SCA map with Sentinel-1 wet snow mask being used to differentiate areas with wet snow. Being able to more accurately map wet snow in SCA maps can contribute to improve hydrological modelling of runoff (Esmaeelzadeh et al. 2024).

Revuelto et al. (2021) used Sentinel-2 and MODIS snow cover observations to increase the resolution from 500m to the 20m of Sentinel-2. The method uses the high-resolution Sentinel-2 snow cover product and applies probabilistic spatial downscaling for the lower resolution MODIS snow cover product. A partially snow-covered pixel from the MODIS snow cover product can be overlaid on the probability mask and increases the resolution from 500m to 20m. Their study showed improved performance of snow cover mapping over the Iberian Peninsula (Revuelto et al. 2021).

Rittger et al. (2021) have examined the possibility to create daily FSC maps with a resolution of 30m by using a random forest algorithm. The method combines data from MODIS and Landsat to overcome the limits of both their spatial and temporal resolution. The 500m spatial resolution of the MODIS data is insufficient for some snow cover applications. Landsat has a similar spatial resolution to that of Sentinel-2 at 30m. By using spectral mixing and a random forest algorithm they were able to create a daily snow cover product of 30m spatial resolution.

## 2 STUDY AREA

The study area that was chosen for the implementation and validation of the snow cover products includes the mountainous parts of Västerbotten county and the northern parts of Jämtlands county in Sweden. See Figure 2 for the exact location. This geographical selection was made strategically to include enough meteorological measuring stations from the Swedish meteorological and hydrological institute (SMHI) as described in section 3.3, which are crucial for the validation of the snow cover products. In conjunction with enough stations and variability in land cover type the available Sentinel-2 FSC tile extent was used to limit the study area within Sweden. 5 tiles that cover the selected SMHI stations are used giving the limit of the study area to the north, east and south. The border between Sweden and Norway was used to limit the extent towards the west.

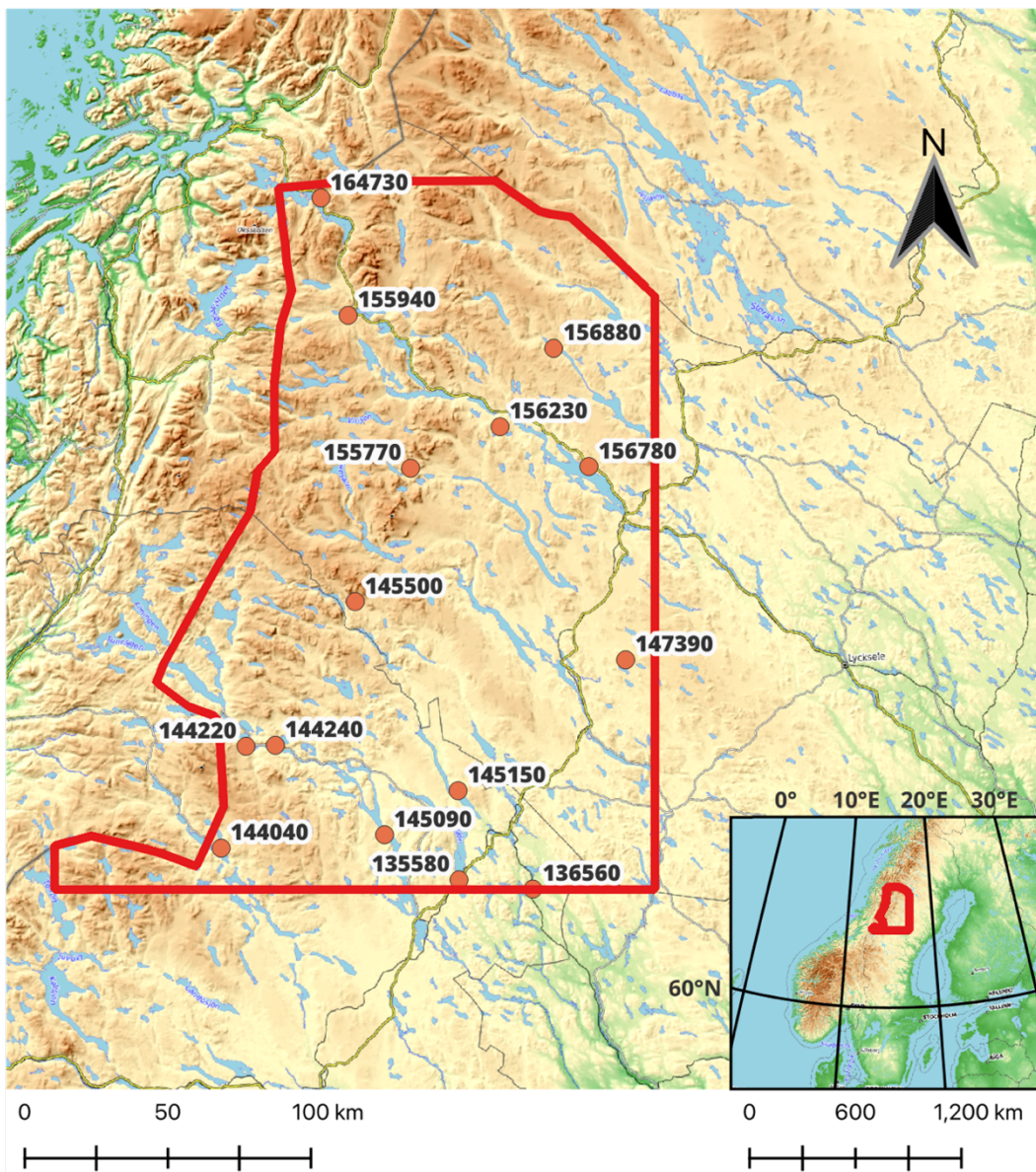


Figure 2: Location of study area outlined with red and location of SMHI meteorological measuring stations within the study area. The western limit of the study area follows the border between Sweden and Norway.

The extent of the area includes a variety of different land cover types to provide an accurate representation of the different environments that exist in the Swedish mountainous areas. The stations located in the western parts towards the Norwegian border are more mountainous whilst the eastern parts are at lower elevation with less topographical variation. The vegetation in the selected area also varies from no to low vegetation at higher elevations in the west to vegetated land and forests (Naturvårdsverket 2023). The variation in land cover type is critical for the selection of the area to make the validation of snow cover products more generalized and applicable to a larger extent of the Swedish mountainous regions.

High enough latitudes experience insufficient light from the sun to facilitate optical observations of the Earth's surface. This phenomenon is called polar darkness and affects parts of the earth at latitudes higher than  $62^{\circ}\text{N}$  (Dietz et al. 2012b). The chosen study area lies above this latitude to include the effects of polar darkness on the examined snow cover products.

### 3 DATA

The following section describes the data used in the study. The two snow cover datasets, Sentinel-2 FSC<sub>OG</sub> and IMS, are presented and explained. The data from the SMHI stations that was used as ground truth data for the validation of the two datasets is presented. The time span that was examined was determined by the availability of Sentinel-2 data since the start of the Sentinel-2 mission is more recent than IMS. The hydrological years of 2018-2023 was used in the study. This means that the 2017-2018 snow season was the first and 2022-2023 snow season was the last used in the study.

#### 3.1 SENTINEL-2 FSC<sub>OG</sub>

The FSC product from the Copernicus Land Monitoring Service (2018) provides a high-resolution snow cover monitoring for the European Union member nations. FSC gives the fraction of a pixel that is covered by snow giving more information than a binary snow not-snow SCE product.

Sentinel-2 consists of a constellation of two satellites, Sentinel-2A and Sentinel-2B, which carry a multi-spectral instrument enabling high resolution multi-spectral images in the visible, near infrared and short-wave infrared region of the spectrum. The spatial resolution varies from 20m to 60m depending on the Sentinel-2 band. Each satellite has a revisit time of 10 days giving the constellation of the two opposing satellites a revisit time of 5 days. At high latitudes even shorter revisit times can be observed since the swath of separate passes overlap (European Space Agency 2024). There are however temporal gaps in the FSC product leading to data gaps with varying temporal resolution (Copernicus Land Monitoring Service 2018)

Cloud detection, atmospheric correction and topographic normalization is first carried out on the Sentinel-2 L1C product using the MAJA algorithm developed by CNES as shown in Figure 3. This resulting product is then used as an input to calculate the NDSI. A second criterion is used with the red band to avoid false snow detection on water surfaces. This modified NDSI algorithm is named LIS by HR-S&I (Gascoin et al. 2019). A first pass through the LIS module is carried out with low thresholds for SCA to estimate regional snowline elevation from a DEM. The second pass uses higher thresholds to refine the snow detection above the established snowline elevation (HR-S&I 2023).

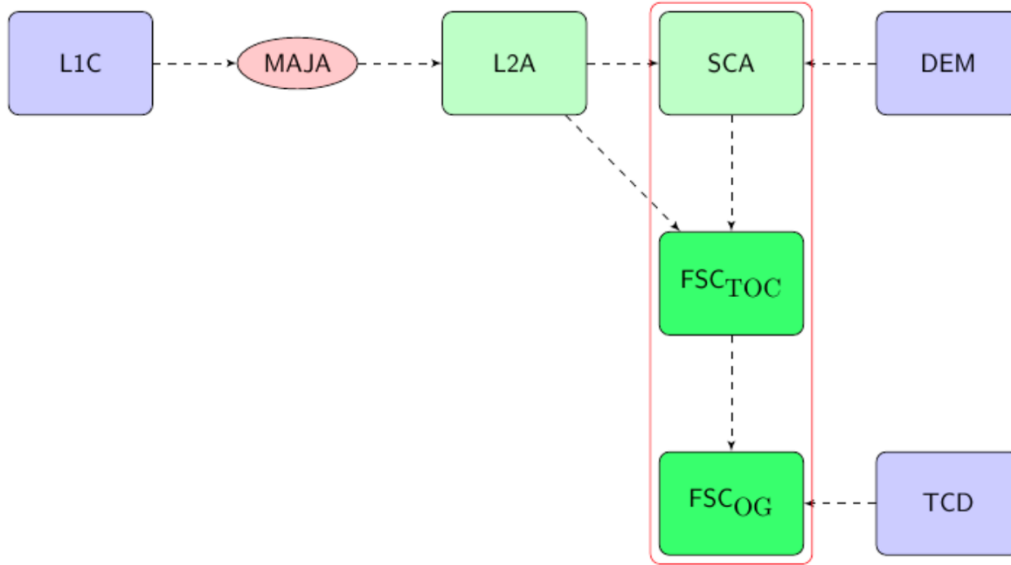


Figure 3: Workflow of the Sentinel-2 FSC algorithm and its intrinsic components. Inputs are presented in purple, intermediate products in light green and outputs in green. The blocks enclosed by the red line indicate parts of the Let it Snow software (LIS) module.

The relationship between NDSI and FSC is established by Salomonson & Appel (2004) for MODIS data. The equation for  $FSC_{TOC}$  is presented in equation ( 1 ). The same function is used for the Sentinel-2 product (HR-S&I 2023) to obtain the FSC.

$$FSC_{TOC} = 1.45 \times NDSI - 0.01 \quad (1)$$

The product is given for FSC on top of canopy ( $FSC_{TOC}$ ) and FSC on ground ( $FSC_{OG}$ ). A viewable gap fraction (VGF) is calculated from the inverse of the tree cover density and used in equation ( 2 ) to adjust the  $FSC_{TOC}$  for the tree cover density at the location. It is recommended to use  $FSC_{OG}$  for snow mapping and it is considered as the final output (HR-S&I 2023). For applications with SCE the  $FSC_{OG}$  can be used as a threshold to create a binary map when  $FSC_{OG} > 0$  (Copernicus Land Monitoring Service 2018).

$$FSC_{OG} = \min (FSC_{TOC} / VGF, 1) \quad (2)$$

The  $FSC_{OG}$  product is provided in tiles of 110km by 110 km for the whole of Europe. With the spatial resolution of the Sentinel-2 satellite, the FS  $FSC_{OG}$  C product is given at a resolution of 20m by 20m (Copernicus Land Monitoring Service 2018). This high resolution allows for detection of snow with high spatial variability. A higher detailed image of the snow cover allows for better accuracy in applications in hydrology, climate studies and water resource management.

Besides the snow cover data, the  $FSC_{OG}$  product also contains a quality information layer which serves to give information about the reliability of the product for each pixel. These are based on several indicators that together creates a confidence index. Sun angle, cloud presence and tree cover density are factors that contribute to a lower confidence index meaning that the pixel value is less reliable (HR-S&I 2023).

For this study a total of 5 tiles was sufficient to cover the study area. The product is distributed in EPSG:32633 coordinate reference system (CRS). The file naming

convention of the  $FSC_{OG}$  product includes a TileID to identify the tiles of each file. A five-character combination of letters and numbers preceded by a capital T. The tiles used in the study were: T33WWM, T33WWN, T33WVM, T33WVP and T33WVN.

The meaning of the values in the Sentinel-2  $FSC_{OG}$  snow cover product are presented in Table 1.  $FSC_{OG}$  represent the FSC on ground and are obtained using equation ( 2 ). Cloud pixels are generated using the MAJA algorithm. Due to overlapping Sentinel-2 acquisition paths some tiles only have partial coverage. As a result, tiles may contain regions with no-data pixels.

Table 1: Description of Sentinel-2  $FSC_{OG}$  snow product values physical meaning.

Value	Description
0-100	$FSC_{OG}$ (%)
205	Cloud of cloud shadow
255	No-data

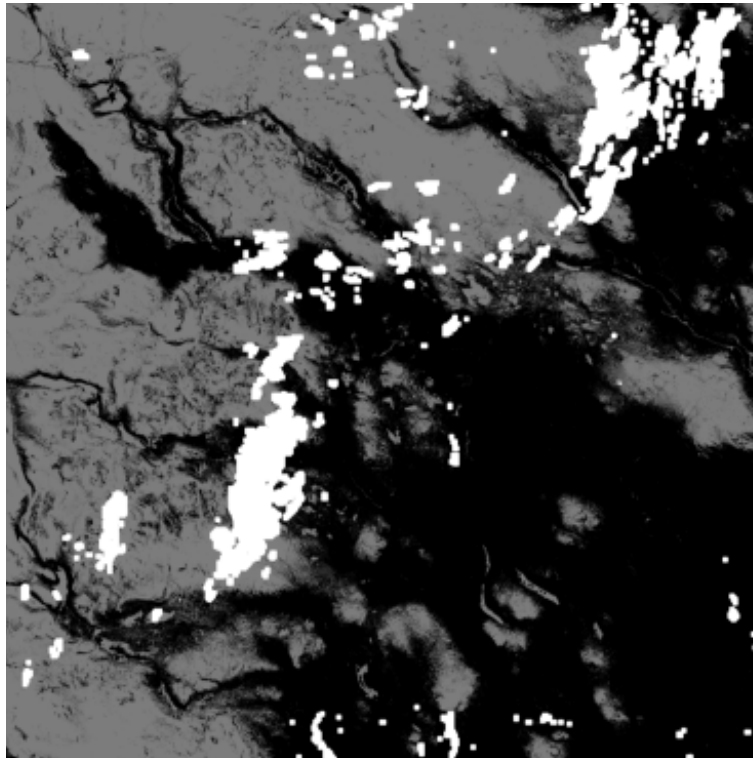


Figure 4: Example of Sentinel-2  $FSC_{OG}$  acquisition from 1 June 2020. In grayscale is the values 0-100 showing the  $FSC_{OG}$  with black indicating 0 and now snow. White shows the value 205 indicating cloud cover. This image does not contain no-data pixels with the value 255.

### 3.2 IMS 1KM

The second snow cover product used in this study is the IMS Daily Norther Hemisphere Snow and Ice Analysis 1km resolution Version 1 (U.S. National Ice Center. 2008). The product is produced by analysts using the Interactive Multisensor Snow and Ice Mapping System (IMS) developed by US National Ice Center (NIC) in collaboration with National Snow and Ice Data Center (NSIDC). It's a software package that combines multiple sources from different sensors allowing analysts to interpret the data and produce daily maps of snow and ice cover on the northern hemisphere (Helfrich et al. 2018).

The system has been developed since 1997 and has seen significant improvements over the years. A predecessor to the IMS product part of the National Oceanic and Atmospheric Administration (NOAA) produced maps a spatial and temporal resolution of 190 km and 7 days by interpreting environmental satellite images. Since the launch of the IMS system in 1997 the snow and ice cover maps have been produced daily at a spatial resolution of 24km. With improvements in computational efficiency and higher resolution satellite imagery a 4km product was introduced in 2004 (U.S. National Ice Center 2008). The 1km product used in this study was released in 2014 and is currently the highest spatial resolution available. This higher resolution product started production after NIC took over production of the IMS software suite (Helfrich et al. 2018).

Input to the model consists of images from several different satellites with sensors such as visible band, passive and active microwave. Polar orbital and geostationary satellites are both used. The analysts prefer visible band images but substitute it for passive microwave when visible images aren't available due to clouds or insufficient light conditions. Other in situ data from several countries are used where they are available. The snow or ice map from the previous day is used as an basis for the current days map (U.S. National Ice Center. 2008).

A land water classification mask is one of the mandatory inputs for the IMS system. It delineates waterbodies and oceans from landmasses. This simplifies distinguishing ice from snow since snow can be classified on top of ice. If an area is classified as snow within region of water determined by the land water mask it will be classified as ice. This acts as a safeguard to only classify water as ice (Helfrich et al. 2018). Lastly a digital elevation model (DEM) is used to better model snow cover in mountainous regions. Topographical changes can then be limits for snow cover allowing the snow to follow the topography. IMS uses the USGS GTPO30 DEM averaged to 1km grid cells (Helfrich et al. 2018)

The production of snow and ice cover images by the IMS consists of four steps. A first step in the pre-processing system is to download all available data for that day through a File Transfer Protocol (FTP). All data is downloaded at the highest resolution of max 1km used for the IMS product. Some data such as microwave have lower resolutions in the region of 20km (Helfrich et al. 2018). The system reprojects each product into the IMS projection to allow analysts to interpret and compare different products. The second step takes each product and displays it in the IMS GUI (graphical user interface) for analysts to interpret. As the third step an analyst tags the locations as snow or ice cover for the whole coverage area. The last step takes the information from the IMS GUI and produces the final product in the various file formats and resolutions that NSIDC distribute (Helfrich et al. 2018).

The process of classifying snow and ice involves the analysts interpreting the state of each 1km grid cell. More than 40% of the cell needs to consist of snow or ice to be classified as such (Helfrich et al. 2018). This is not a threshold applied to any of the input data per se but rather the combined evaluation of all the different data sources available for the area (U.S. National Ice Center. 2008). In the 1km product some cells can be combined into 4km cells if half or more of the 1km cells in a 4x4 area has the same class (Helfrich et al. 2018).

The IMS 1km product is ultimately produced by analysts applying their expert knowledge to determine the snow or ice state of the surface. There are few algorithms running for this classification other than reprojecting and converting the data correct formats and displaying it for the analysts (Helfrich et al. 2018).

The IMS product is distributed in different resolutions and formats suitable for various applications. From 24km to the one used in this study of 1km. Among the different formats GeoTIFF was chosen for this project because of its compatibility with common GIS software. The product is distributed in a polar stereographic projection. The area covered by the IMS snow cover product contains the whole northern hemisphere. The product was acquired through the NSIDC HTTPS file system(U.S. National Ice Center 2004). The values in the IMS GeoTIFF files represent different classes according to Table 2.

An example acquisition of the IMS snow cover product is shown in Figure 5. White represents the value 4, snow covered land. Light grey shows the value 3, sea ice. Dark grey illustrates the value 2, land without snow. Lastly black illustrates the value 1, open water.

Table 2: Description of IMS 1km snow product values physical meaning (U.S. National Ice Center 2004).

Value	Description
0	Outside coverage area
1	Open water
2	Land without snow
3	Sea ice
4	Snow covered land

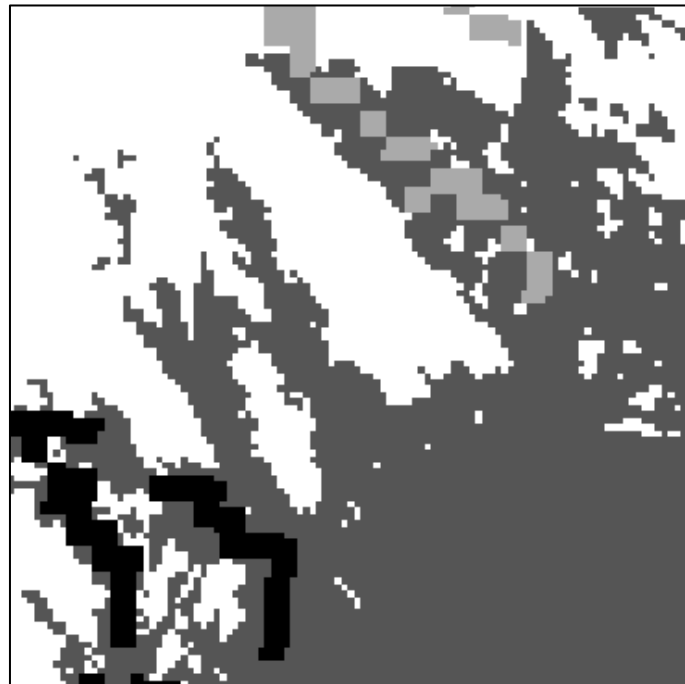


Figure 5: Example acquisition of IMS snow cover product from 20 May 2020. White represents the value 4, snow covered land. Light grey shows the value 3, sea ice. Dark grey illustrates the value 2, land without snow. Lastly black illustrates the value 1, open water.

### 3.3 SMHI

In situ measurements from the Swedish Meteorological and Hydrological Institute (SMHI) were used as ground truth data. SMHI manages several weather stations throughout Sweden where snow depth measurements are taken every day. The data is freely available to download from their website. The stations use a measuring stick placed on the ground to measure the snow depth. Measurements are conducted when more than half of the sample area is covered by snow (SMHI 2024). Along with snow depth in meters a code for the state of the ground is also included following a set of codes established by SMHI. The codes range from 0-19 with the codes 12-14 and 16-19 indicating the presence of snow on the ground (SMHI 2024). The codes used in this study represent snow descriptions described in Table 3.

Table 3: SMHI code convention of snow cover types based on their coverage and characteristics (SMHI 2024).

Code	Description
12	Partly or completely covered of packed or wet snow – at least 50 % but not completely.
13	Partly or completely covered of packed or wet snow – completely in an even layer.
14	Partly or completely covered of packed or wet snow – completely in an uneven layer.
16	Partly or completely covered of loose and dry snow – at least 50 % but not completely.
17	Partly or completely covered of loose and dry snow – completely in an even layer.
18	Partly or completely covered of loose and dry snow – completely in an uneven layer.
19	Completely covered by snow with high snowdrift.

The remaining codes indicate other types of ground state such as frost, flooded and sand. These categories were deemed irrelevant for the project and were thus not used and not described here.

Stations located within the study area, that provided continuous time-series data from the start of the Sentinel-2 mission to the conclusion of the 2023 snow season, were selected as sources of ground truth data. This resulted in the following 15 stations:

Table 4: SMHI meteorological stations used in the study. Each station is identified by a unique station ID. The latitude and longitude of the station was used to make geographical analysis of the data from each station (SMHI 2024).

Station ID	Name	Latitude	Longitude
135580	Lövberga	63.9673	15.8437
136560	Rossön	63.9338	16.3694
144040	Valsjöbyn	64.0655	14.1433
144220	Frostviken	64.3854	14.314
144240	Fågelberget	64.3892	14.5262
145090	Hillsand	64.8395	15.1065
145150	Kyrktåsjön	64.2454	15.8454
145500	Avasjön-Borgafjäll	64.8395	15.1065
147390	Latikberg	64.6425	17.0833
155770	Kittelfjäl	65.2559	15.5229
155940	Mosekälla	65.7346	15.056
156230	Bastansjön	65.3817	16.197
156790	Baliken	65.2506	16.8563
156880	Fjällsjönäs	65.6229	16.6157
164730	Mjölkbacken	66.1020	14.8465

The data from the stations varied in terms of continuity. In the data from some stations, gaps were detected where no data was recorded. The reason for this is unknown but could be due to technical issues or maintenance that disrupted the data collection. These discontinuities mean that some of the conducted analyses couldn't be performed for these stations due to the analysis requiring continuous data.

## 4 METHOD

### 4.1 VALIDATION SENTINEL-2 AND IMS SNOW COVER PRODUCTS

A comprehensive validation between ground truth in situ measurements and snow cover products from remote sensed data was conducted to evaluate the respective products. By comparing the snow cover products to in situ snow depth measurements it's possible to determine the accuracy of the products in the study region (Klein & Barnett 2003; Dietz et al. 2012b; Gascoin et al. 2019; Chen et al. 2012).

The entirety of the validation was done in Python. The Python modules Rasterio, GDAL, pandas, GeoPandas and Shapely was specifically used to handle raster images and geographical data.

#### 4.1.1 Station data extraction for validation

Data from 15 SMHI snow monitoring sites was use as ground truth data and compared to data from the different snow cover products. Sentinel-2 FSC<sub>OG</sub> and IMS 1km snow cover products are both provided as raster data covering the whole study area. For the validation the coordinates of the stations were reprojected to each products CRS to ensure accurate comparison. The raster value for each product at the coordinates of the stations was then used to extract the snow cover information for all days where data was available. The analysis was done in Python using Pandas dataframes for managing the data, Rasterio and GDAL for raster operations and GeoPandas for geographical tubular data.

To make a valid validation the data had to be filtered to only compare the snow cover product to the data from stations on days with clear sky. Therefore, acquisitions from the Sentinel-2 snow cover product that had clouds obscuring the stations were removed from the validation. The IMS product is not sensitive to cloud cover and can be used without needing to remove cloud cover (U.S. National Ice Center. 2008). The coarse resolution in the IMS product does however cause problems with stations close to waterbodies. Stations close to lakes can be misclassified as waterbodies in the IMS snow cover product. These stations that consistently were classified as waterbodies were removed from the validation to better represent the accuracy of the snow detection and not waterbodies.

The validation was then performed for each station and day with available data. At each day the value of the Sentinel-2 FSC<sub>OG</sub> and IMS snow cover product was recorded as well as the SMHI station data. The result of the validation was a tabular dataset containing the snow cover information of each examined data source. The data of the snow cover is in binary form of snow or non-snow. The Sentinel-2 FSC<sub>OG</sub> snow cover product was converted from FSC to binary snow cover product by using a threshold of above 0 being classified as snow.

#### 4.1.2 Statistical metrics for station based validation

The new dataset produced in the previous chapter contains the ground truth data from the SMHI dataset and the predicted data of the Sentinel-2 FSC<sub>OG</sub> and IMS snow cover products. The classes are snow or non-snow represented by the values 1 and 0 in the

dataset. To evaluate the accuracy of the snow cover product several statistical measurements commonly used to evaluate classification models were used.

The accuracy measures how well a model classifies all instances correctly. It is calculated as the ratio of the sum of correctly classified true positives and true negatives and the total amount of instances (Kulkarni et al. 2020).

$$Accuracy = \frac{TP + TN}{TP + TN + FP + FN} \quad (3)$$

A true positive (TP) is in this case when both the ground truth data and predicted data are snow or as it is represented in the data the value 1. True negative (TN) is when both are non-snow or the value 0. False positive (FP) and false negative (FN) are cases where the predicted values do not match the ground truth.

Precision of a model measures how many of the positive predictions that are correct. It gives an indication of how accurate the positive predictions are (Kulkarni et al. 2020). For snow cover classification it indicates how many of the predicted instances of snow cover contained snow.

$$Precision = \frac{TP}{TP + FP} \quad (4)$$

Recall or sensitivity of a model measure the ratio of positive instances that the model correctly classifies. It helps to asses if the model misses any positive instances (Kulkarni et al. 2020). For snow cover classification it explains how many of the instances of snow according to the ground truth that the model predicted as snow. A low recall means that the model missed many instances of snow.

$$Recall = \frac{TP}{TP + FN} \quad (5)$$

F1-score is the harmonic weighted mean of both precision and recall. It is used as a measurement for evaluating the balance between how correct the model is versus how much it covers (Kulkarni et al. 2020).

$$F1 = 2 \times \frac{precision \times recall}{precision + recall} \quad (6)$$

A confusion matrix is a statistical tool to evaluate the performance of a classification model. It gives an overview of the model's predictions. This allows for an understanding of what the inaccuracies in the models predictions are (Kulkarni et al. 2020). As the famous quote goes; "All models are wrong, but some are useful" (Box 1979), it is important to understand how a model behaves and if it has a bias or variation. For classification models the confusion matrix is tool for that. Confusion matrixes for validation and intercomparison of snow cover models have previously been used for the algorithm behind the Sentienel-2 FSC<sub>OG</sub> snow cover product and MODIS snow cover product (Gascoin et al. 2019; Klein & Barnett 2003).

The amount of TN, FN, FP and TP that a model makes are presented in a confusion matrix, see Figure 6 for an example of a binary confusion matrix. A perfect model would generate no FP or FN and have all the instances in TN and TP. This can be seen in the confusion matrix as the false classified instances lies outside of the diagonal in the matrix.

		Negative	Positive
		Negative	TN
True	Positive	FN	TP
			Predicted

Figure 6: Example of a binary confusion matrix for classifications with positive and negative instances. Predicted values from a model and true values that the predicted values are compared to.

Due to the different temporal resolution of the Sentinel-2 FSC<sub>OG</sub> and IMS snow cover products, they have varying amounts of snow and non-snow instances in their datasets. This inconsistency makes it challenging to directly compare the confusion matrixes of the two products. To address this issue, the confusion matrixes were normalized according to a method described by Hardin & Shumway (1997). By normalizing the confusion matrices, the ratio of predictions can be presented within the confusion matrix instead of absolute numbers.

#### 4.2 CLOUD IMPACT ANALYSIS OF SENTINEL-2 SNOW COVER PRODUCT

Cloud cover is one of the main limitations in remote sensing of snow cover. Areas with clouds cover inhibit a clear view of the ground and no light in the spectrum relevant for snow detection can pass through clouds and reach a sensor in space. Several studies have previously attempted to limit the influence of cloud cover in snow cover products from the MODIS (Gafurov & Bárdossy 2009, Parajka & Blöschl 2008, Wang et al. 2008). The snow cover product from Sentinel-2 faces similar limitations as the MODIS product (Copernicus Land Monitoring Service 2018). To better understand and quantify the impact of cloud cover on the Sentinel-2 snow cover product, an analysis of the frequency of cloud-covered days at each SMHI station was conducted. This analysis aimed to determine how often cloud cover obstructs snow detection in the Sentinel-2 imagery. The analysis was implemented using Python, with Pandas dataframes employed to manage and process the data efficiently. By assessing the extent of cloud cover, the aim is to highlight the challenges in snow cover detection and propose potential strategies for improving data accuracy under cloudy conditions.

The cloud impact analysis was performed for each SMHI station. To calculate the number of cloud days in the Sentinel-2 FSC<sub>OG</sub> data at each station the value 255 which indicates cloud cover was used. The number of days with 255 was then used as the total number of cloud cover days for each station. By grouping each day of the year and calculating the sum for each group, the cloud cover for each day could be calculated. Because of the gaps in the Sentinel-2 data due to cloud cover and insufficient

illumination, the distribution of acquisitions is uneven through the year. Some days have therefore more acquisitions than other. To better show the distribution of cloud cover during the year, the amount of cloud cover days was normalized by the number of acquisitions for each day of the year. The data for each month was then grouped together and averaged to display the mean percentage of days impacted by cloud cover for each month.

To analyze the ratio of individual pixels that are unusable because of clouds a point-based analysis of the whole dataset was conducted. An algorithm that counted all the pixels in the FSC<sub>OG</sub> product with the value 205 (clouds) and 255 (no-data) (Copernicus Land Monitoring Service 2018). To ensure the accuracy of the dataset, the count of pixels was conducted separately so that pixels with no data could be excluded from the total pixel count. Additionally, a count of the total number of pixels in the dataset was performed. Using these counts, the ratio of individual pixels classified as clouds was then calculated according to equation ( 6 ).

$$\text{Ratio of cloud pixels} = \frac{\text{Cloud pixels} - \text{nodata pixels}}{\text{total pixels} - \text{nodata pixels}} \quad (6)$$

The ratio of cloud pixels in the Sentinel-2 FSC<sub>OG</sub> dataset gives an indication of how much of the data is usable for snow cover mapping. This information was used to compare the original product to the one created in this study.

Lastly an analysis of the whole FSC<sub>OG</sub> dataset was conducted to count the number of acquisitions for each month regardless of cloud cover or the value given by the snow product. This was meant to illustrate how the temporal distribution of the product is spread out across the year. This have previously been done for the MODIS snow cover product to evaluate the cloud cover percentage across Europe (Dietz et al. (2012b).

### 4.3 SNOW COVER DYNAMICS

Two snow cover dynamics parameters were considered for the two snow cover products Sentinel-2 FSC<sub>OG</sub> and IMS. These parameters indicate how well the snow products are at describing the seasonal trends of the snow cover at the stations. The parameters are important for climate studies to track changes in snow cover trends as well as in hydrological modelling. Binary snow cover data limits the parameters that can be observed. For example, it is not possible to calculate the maximum height of the snow cover since no snow depth data is available for the snow cover products in this study. Snow cover onset and end date as well as snow cover duration are therefore chosen as the snow dynamic parameters to be investigated in this study. The analysis was done in Python using Pandas dataframes for managing the data.

#### 4.3.1 Snow cover onset and end date

For each station and year, the first observation of snow cover in the hydrological year was determined to be the SCOD. Subsequently the last observed day with snow cover in the hydrological year was determined to be the SCED (Klein et al. 2016). This was done with the point data from the validation of the snow cover products. To calculate the SCOD for each hydrological year a filter for each year and station was used to separate the dataframe into partitions of station and year. Then the first day with snow cover was saved in another dataframe with information about the year, station number, longitude, latitude and the SCOD. For the SCED the same procedure was done and the last day in

the hydrological year with snow cover was saved to the new dataframe. The new dataframe then contained the SCOD and SCED for each year and stations. The mean of SCOD and SCED for each station across all years was calculated. The difference for each snow cover product and SMHI validation data was then calculated to determine the combined accuracy of the SCOD and SCED for each product.

#### **4.3.2 Snow cover duration**

Snow cover duration (SCD) is calculated by counting the number of days with snow cover during the hydrological year. It is measured in days and has a maximum value of 365 or 366 days for areas with persistent snow cover such as glaciers (Dietz et al. 2012b). Before the SCD could be calculated it was necessary to apply a gap filling method for the Sentinel-2 FSC<sub>OG</sub> snow cover product due to the significant gaps in the acquisitions because of Sentinel-2's low temporal resolution. A technique previously used with the MODIS snow cover product (Gafurov & Bárdossy 2009; Dietz et al. 2012b) was applied to the Sentinel-2 FSC<sub>OG</sub> snow cover product to fill in the gaps between acquisitions. The method utilizes a forward fill method which compares the day with no data (either by no acquisition of cloud cover) with the previous day and uses that value (Gafurov & Bárdossy 2009). This simple method carries the last observed snow cover value forward until a new, valid data is acquired. This creates an uninterrupted timeseries of the snow cover from the Sentinel-2 snow cover product.

The data used for the calculations of the SCD was the same as in the calculation of SCOD and SCED. First the forward fill method was performed on the dataframe to create a continuous dataset. For each station and years, the number of days in each hydrological year with snow cover was then calculated. Since the snow cover was binary with snow cover having the value 1 this was easily done by calculating the sum of the snow column for each year which gives the SCD. The SCD was then saved in a new dataframe along with station number, longitude, latitude and year. The mean SCD for each station across all years was calculated and then compared to the SMHI validation data to determine the SCD accuracy of the snow products.

#### **4.4 SENTINEL-2 AND IMS SPATIOTEMPORAL FUSION ALGORITHM**

The algorithm for the spatiotemporal fusion integrates the high spatial resolution Sentinel-2 FSC<sub>OG</sub> snow cover product and the high temporal resolution IMS snow cover product to create an improved gap-free snow cover product with good spatial and temporal resolutions. This method aims to mitigate the limitations of each product by combing their separate strengths to provide a more detailed and comprehensive monitoring of the snow cover. The method draws inspiration from Rittger et al. (2021) to use a high resolution snow cover dataset in combination with a daily lower resolution snow cover dataset to create a better snow cover product. The algorithm here utilizes a more simple change detection (Hecheltjen et al. 2014) of the IMS as the input for extrapolating the Sentinel-2 FSC<sub>OG</sub> data.

The algorithm begins with initializing the directories for the Sentinel-2 FSC<sub>OG</sub> and IMS datasets. The files are moved to the directories and named to the same naming convention of *type\_year\_dayofyear\_code*. Type is either FSC or IMS depending on the dataset. This code was only used for the FSC<sub>OG</sub> dataset to separate the different Sentinel-2 tiles into groups for easier access and more efficient processing. The IMS and FSC<sub>OG</sub> products are provided in different CRS. Before any fusion of the two was performed they need to have the same CRS to ensure the images align geographically.

The lower spatial resolution of the IMS product resulted in the images having fewer pixels which makes reprojection less computationally expensive. The IMS product was therefore reprojected to match the CRS of FSC<sub>OG</sub>, EPSG:32633. Since the IMS product contains the whole northern hemisphere only a small part was needed to cover the study area. A mask was applied to the images to extract and save only the area covered by the study area. The steps ensured that the data was prepared and stored in a format that fits the fusion algorithm.

A separation of the dataset was made with the codes allowing each code and its corresponding Sentinel-2 FSC<sub>OG</sub> tile to be processed in parallel. This was done to speed up the run time of the code by using the multiple threads available on in the CPU on the laptop that was used. Similar strategies have been proposed by Zhu et al. (2018) to improve the efficiency of spatiotemporal fusion algorithms.

The main part of the algorithm iterates through each day during a time interval set by the user. The scheme follows the logic described next and illustrated in Figure 7. If the current day has an acquisition from the Sentinel-2 FSC<sub>OG</sub> product that image is then used in the new dataset and the algorithm proceeds to the next day. That essentially copies the existing FSC<sub>OG</sub> product. In the cases where there is no Sentinel-2 FSC<sub>OG</sub> on the current day, the fusion part is applied. The algorithm calls for a function to calculate a difference mask between two IMS images, the first IMS from the current day and the other from the following day. The resulting difference mask provides information about the change in snow cover that has occurred between the two days according to the IMS dataset. It can be both increase in snow from snowfall or snow drift or decrease in snow from melting of the snowpack. The mask is binary and has pixels of value 1 where there is a difference in the snowpack and 0 where no change has occurred.



used instead. This continues until a new  $FSC_{OG}$  is detected for the current day. The process then repeats for each day throughout the specified time interval.

A new dataset was created using the algorithm with a gap limit of 2 days. This dataset is named V2, referring to it both being version of the Sentinel-2 product and having a gap limit of 2 days. After 2 days without new  $FSC_{OG}$  images the IMS images are used instead. The new images in the new dataset are saved as GeoTIFF files with geographical metadata of the projection from the  $FSC_{OG}$  images. LZW compression in the GDAL write function was used to reduce the file size of the images in the new dataset. This compression algorithm is lossless which was important since the precision of the data is crucial to accurately map the snow cover.

#### **4.5 VALIDATION OF NEW V2 DATASET AND COMPARISON TO SENTINEL-2 $FSC_{OG}$**

The validation for the new product was conducted for the new dataset V2 in the same manner as described in Section 4.1 for the Sentinel-2  $FSC_{OG}$  snow cover product. The new product was compared to the SMHI ground truth data to measure the statistical metrics accuracy, precision, recall and F1-score as in Section 4.2. The same snow dynamic metrics as in Section 4.3 were also calculated for the new dataset.

## 5 RESULTS

Presented in part 1 are the results from the validation with the snow cover products Sentinel-2 FSC<sub>OG</sub> and IMS to SMHI data. The validation was done for the study area presented in section 2 and SMHI data from the stations presented in section 3.3. The results from the validation of the new dataset, referred to as V2, generated by the spatiotemporal fusion algorithm described in the previous section, are presented in Part 2. Additionally, examples of snow cover maps derived from the new dataset are provided to illustrate the effectiveness and accuracy of the developed algorithm. A gap limit of 2 days was used in the algorithm for the validation. An additional dataset with a gap limit of 5 days was used for pixelwise cloud analysis to evaluate the parameters effect on the available data.

### 5.1 POINT BASED VALIDATION OF SENTINEL-2 AND IMS SNOW COVER PRODUCTS

In this section the results from the validation of Sentinel-2 FSC<sub>OG</sub> and IMS snow cover products are presented. 5 SMHI stations are excluded for the validation of the IMS product since the water mask in the IMS product consistently classifies these stations as ice or water. Therefore, only 10 stations were used for the validation of the IMS product compared to 15 stations for the Sentinel-2 FSC<sub>OG</sub> product. The excluded stations were stations 144040, 144220, 144240, 145090 and 164730.

In the Sentinel-2 FSC<sub>OG</sub> dataset no data is produced and distributed when there is insufficient illumination as there is in the winter months. No information about the cloud cover during this period is thus also not available. To show the effect of this the distribution throughout the year of all the available Sentinel-2 FSC<sub>OG</sub> acquisitions for the whole study area are shown in Figure 8. The figure illustrates how big percentage of the distributed data is available for each month. The figure shows the average for the whole study period. This shows which months had the most acquisitions and which had the least. Most acquisitions during the study period happened in the months February, March, April and May. December had no acquisitions and January had the lowest number of acquisitions. This shows the lack of acquisitions during the critical winter months of the snow season where snow is present.

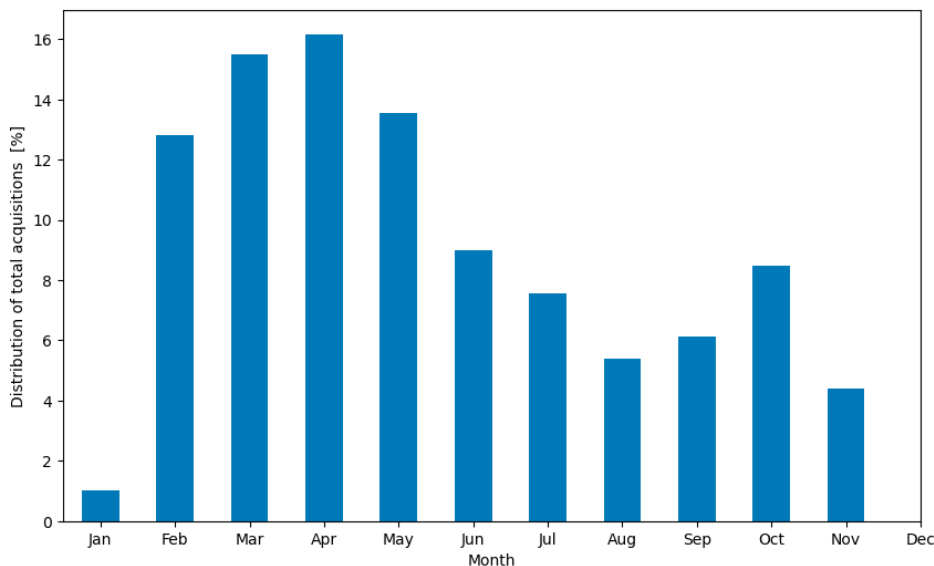


Figure 8: Distribution of FSC<sub>OG</sub> acquisitions throughout the year. The distribution of total acquisitions for all the Sentinel-2 FSC<sub>OG</sub> acquisitions on the y-axis and month on the x-axis

The validation of the two snow cover products produced an initial confusion matrix which values are presented in Table 5. In Figure 9 are the normalized confusion matrixes for the validation of snow cover products evaluated on the SMHI ground truth data. The values are normalized by dividing the values with the total number of comparisons for each snow cover product. For each confusion matrix, the comparisons of snow and non-snow classifications sum to 1. 94% of the comparisons between FSC<sub>OG</sub> and SMHI were correctly classified as snow cover. 97% were correctly classified as bare ground. 3% were incorrectly classified by FSC<sub>OG</sub> as snow when there was no snow present according to the ground truth data. 6% were incorrectly classified as bare ground when snow cover was present according to the ground truth data. 97% of the comparisons between IMS and SMHI were correctly classified as snow cover. 89% were correctly classified as bare ground. 11% were incorrectly classified by FSC<sub>OG</sub> as snow when there was no snow present according to the ground truth data. 3% were incorrectly classified as bare ground when snow cover was present according to the ground truth data.

Table 5: Validation of Sentinel-2 FSC<sub>OG</sub> and IMS snow products. Total number of TP, TN, FP and FN for each product.

Confusion Metric	Sentinel-2 FCS <sub>OG</sub>	IMS
True Positive	1730	9645
True Negative	1589	5396
False Positive	52	668
False Negative	111	275

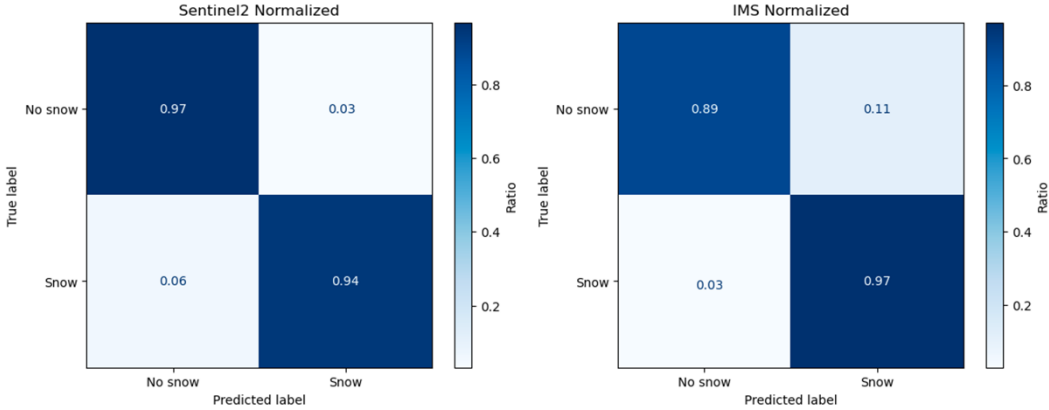


Figure 9: Confusion matrix of Sentinel-2 FSC<sub>OG</sub> and IMS snow products evaluated against SMHI ground truth data. Values normalized to account for the number of acquisitions per snow product. The values represent the ratio that the snow products were either TN in top left, FP top right, FN lower left and TP lower right.

Presented in Table 6 are the calculated statistical metrics for each snow cover product from the validation on the SMHI ground truth data. Sentinel-2 FSC<sub>OG</sub> show higher values for accuracy, precision and F1-score while IMS had higher recall.

Table 6: Metrics from the validation of the snow cover products compared to the SMHI ground truth data. Sentinel-2 FCS<sub>OG</sub> on in the middle and IMS on the right. The accuracy, precision, recall and F1-score are presented for both the snow products.

Metric	Sentinel-2 FCS <sub>OG</sub>	IMS
Accuracy	0.95	0.94
Precision	0.97	0.94
Recall	0.94	0.97
F1-Score	0.96	0.95

## 5.2 CLOUD IMPACT ANALYSIS OF SENTINEL-2 FCS<sub>OG</sub> SNOW COVER PRODUCT

The analysis of the Sentinel-2 FCS<sub>OG</sub> cloud cover at the stations is presented in the following section. Presented in Figure 10 are the percentage of data loss due to cloud cover for each month in the Sentinel-2 FCS<sub>OG</sub> dataset for all stations combined. For most months around 40% of the available data is unusable due to cloud cover. The month in the Sentinel-2 FCS<sub>OG</sub> dataset with most days obscured by clouds was October. The month with the least days obscured by clouds was July.

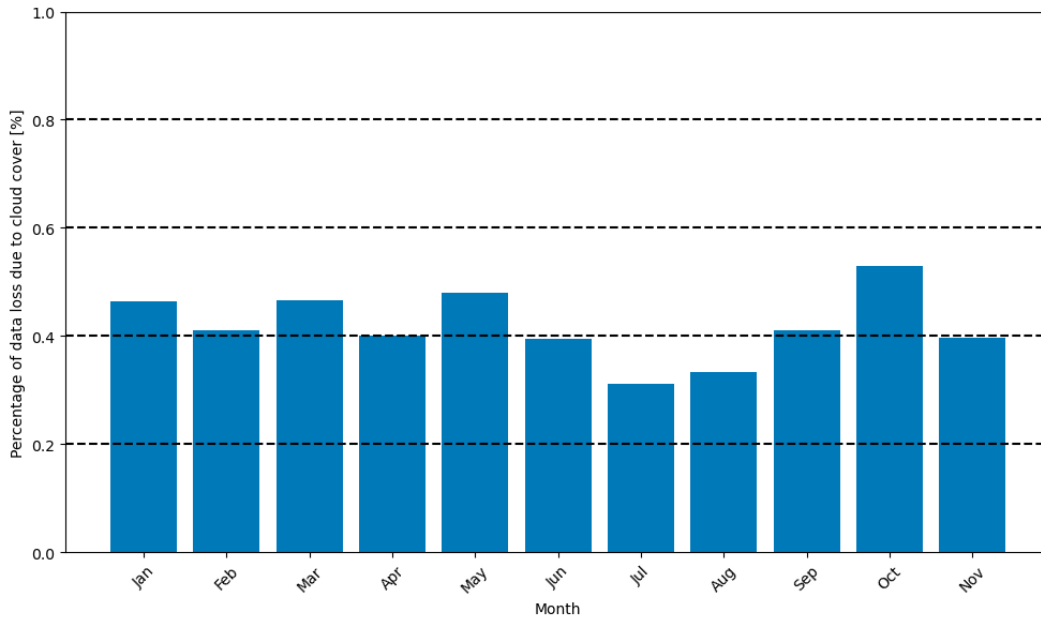


Figure 10: Percentage of data loss due to cloud cover for all stations, aggregated for each month in the Sentinel-2 FCS<sub>OG</sub> snow cover product.

In Figure 11 the yearly percentage of data loss due to cloud cover are presented for each station. Each color represents a different SMHI station. The pixelwise percentage of data loss due to cloud presence for the whole Sentinel-2 FCS<sub>OG</sub> dataset was 48.8%. This percentage considers all the pixels in the images and not only the pixels at the SMHI stations. Station 136560 showed 100% data loss in 2017 due to there only being one acquisition available in that year which in turn was unusable because of cloud cover.

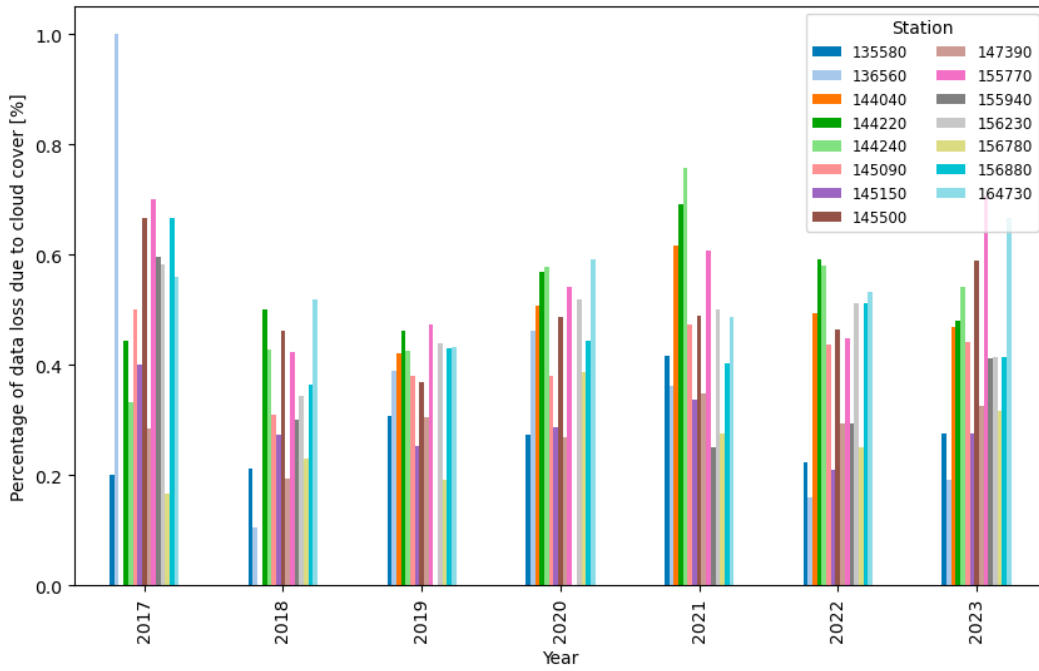


Figure 11: Percentage of data loss due to cloud cover at all stations for the Sentinel-2 FSC<sub>OG</sub> snow cover product. Each year is grouped together on the x-axis.

Figure 12 shows a scatter plot of the relationship between cloud cover days with longitude and latitude. The longitudes range from 14 to 17 degrees east and the latitudes range from 64 to 66 degrees north which is within the study area. A negative correlation between cloud cover and longitude is observed for the Sentinel-2 FSC<sub>OG</sub> product with a  $R^2$  value of 0.49. No correlation was observed when compared to latitude because of the low  $R^2$  value.

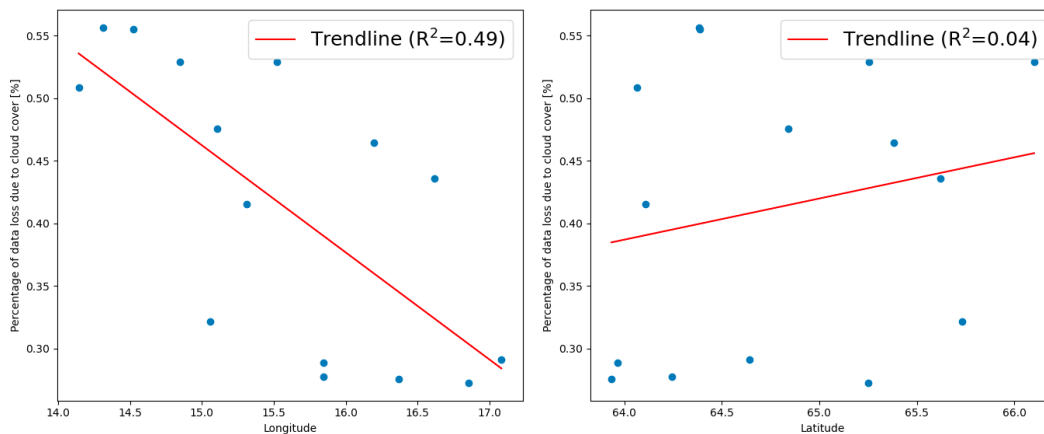


Figure 12: Percentage of data loss due to cloud cover at each station for the Sentinel-2 FSC<sub>OG</sub> product averaged across all years. Presented here with the latitude (to the left) and longitude (to the right) of the stations.  $R^2$  of 0.49 when plotted against longitude and  $R^2$  of 0.04 when plotted against latitude.

### 5.3 SNOW COVER DYNAMICS FROM SENTINEL-2 AND IMS SNOW COVER PRODUCTS

In this section the snow cover dynamics from the validation are presented. The results shown here 10 stations (or latitudes as the stations are represented here) for Sentinel-2 FSC<sub>OG</sub> and therefore less than the total 15 stations that were used in the study. Several of the SMHI stations had long gaps in the snow data. Without consistent data of the snow cover it is not possible to calculate the accurate snow dynamic metrics. Therefore, stations 136560, 144040, 144220, 145090 and 155940 were excluded from the validation. For IMS the stations 144240

and 164730 are also excluded since previously because of them being classified as water or ice. The forward fill method described in section 4.3.2 was used to make the Sentinel-2 FSC<sub>OG</sub> data continuous which was needed for calculating SCD.

Figure 13 illustrates the relationship between snow cover days and latitude. The snow cover days for each station (represented in the figure by their corresponding latitudes) are aggregated across all years and the average is presented here. More snow cover days were observed by the IMS snow cover product as compared to the Sentinel-2 FSC<sub>OG</sub> snow cover product. Higher amount of snow cover days is observed at higher latitudes. The average absolute difference between the Sentinel-2 FSC<sub>OG</sub> data and SMHI data was 19.4 days. The average absolute difference between the IMS data and SMHI data was 7.4 days.

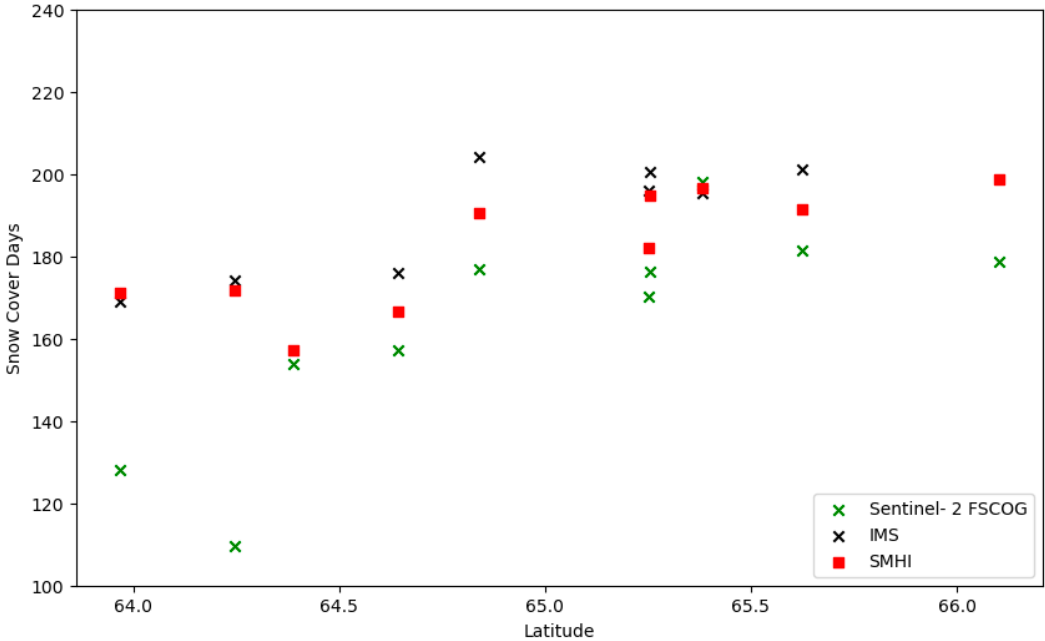


Figure 13: Comparison of snow cover days as a function of latitude. Each year is aggregated for the stations and the mean is presented. On the x-axis is the SMHI station latitude. SMHI ground truth data in red, IMS in black crosses and Sentinel-2 FSC<sub>OG</sub> in green crosses.

The SCOD and SCED for the snow products and the SMHI data is presented in Figure 14. The hydrological year starts at the bottom of the y-axis. SMHI stations are represented on the x-axis by their latitude. Longer snow seasons are observed for higher latitudes. The average absolute difference between the Sentinel-2 FSC<sub>OG</sub> data and SMHI data was 21.1 days. The average absolute difference between IMS data and SMHI data was 10.3 days.

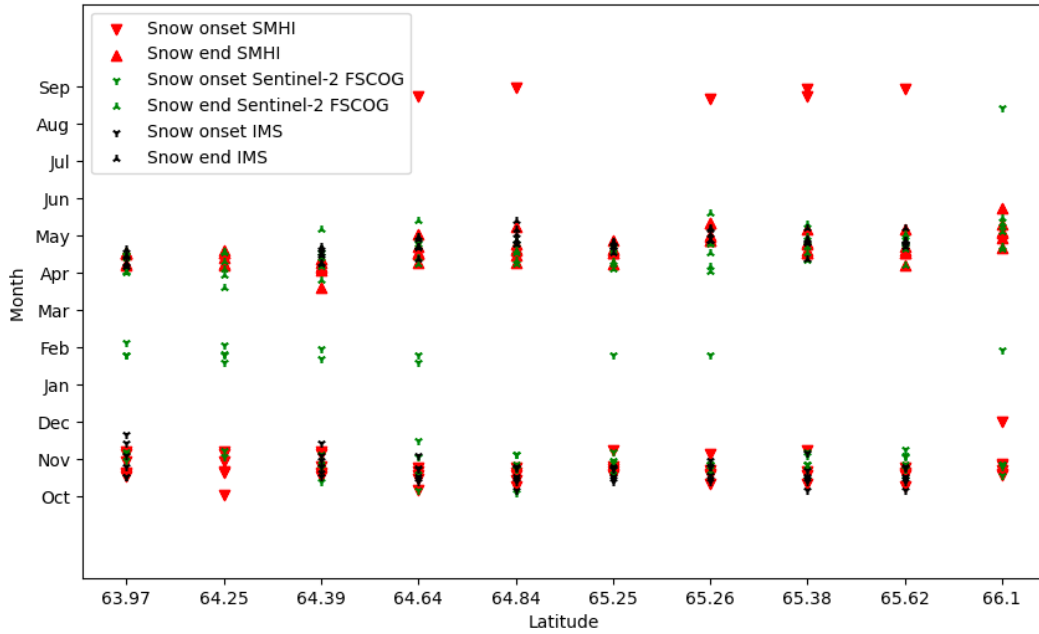


Figure 14: Snow onset and snow end dates for the snow cover products and SMHI ground truth data. Onset is presented with downward-pointing markers, while end is presented with upward-pointing markers. On x-axis is the SMHI station latitude. SMHI values in red, Sentinel-2 FSCOG in green and IMS in black.

#### 5.4 STATION BASED VALIDATION OF V2 DATASET FROM SPATIOTEMPORAL FUSION ALGORITHM

In this section the results from the validation of the new V2 dataset from the spatiotemporal fusion algorithm is presented. The data is validated against the SMHI ground truth data. Figure 15 show the distribution of the available V2 snow cover data throughout the year. The values are an aggregation for all the years of the study period. This shows how large of a percentage of the acquisitions that occur for each month. The summer months of June, July and August show the least amount of available snow cover data. The distribution of the acquisitions is roughly equal throughout the year. The V2 snow cover product has data even during the months with polar darkness.

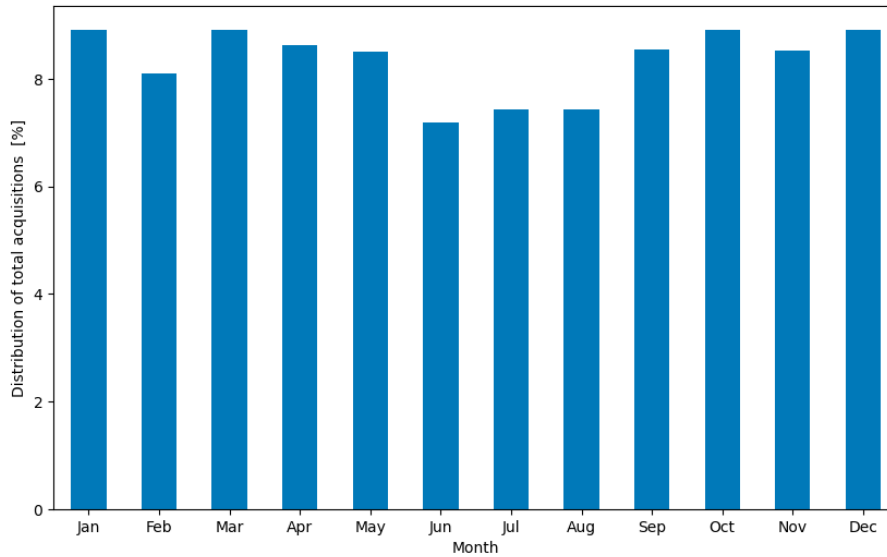


Figure 15: Distribution of available V2 acquisitions throughout the year. The distribution of total acquisitions for all the V2 acquisitions on the y-axis and month on the x-axis

The V2 snow cover product had a total of 26 809 comparisons made with the ground truth data. 12 762 of these were correctly classified as snow cover. 11 335 were correctly classified as bare ground. 941 were incorrectly classified by FSC<sub>OG</sub> as snow when there was no snow present according to the ground truth data. 1771 were incorrectly classified as bare ground when snow cover was present according to the ground truth data. Figure 16 shows the normalized confusion matrixes from the validation. For validation data for each individual station see Appendix 9.1.3. The normalized confusion metrics were 88% TP, 92% TN, 8% FN and 12% FP.

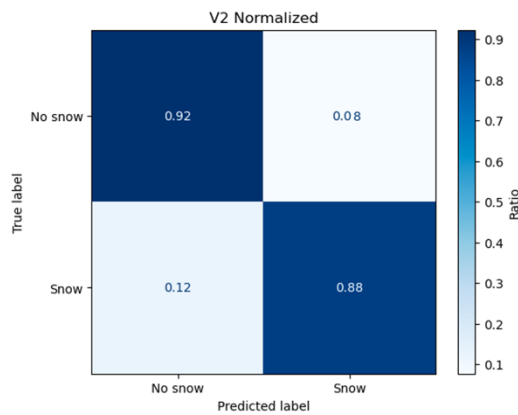


Figure 16: Normalized confusion matrix of V2 snow cover product evaluated on SMHI Ground truth data. TN in top left, FP top right, FN lower left and TP lower right. The values are normalized to account for the number of acquisitions per snow product.

Presented in Table 7 are the calculated statistical metrics for the V2 snow cover product from the validation on the SMHI ground truth data. All the metrics are lower for the V2 snow cover product compared to those from the original snow cover products. The V2 product had a higher precision than recall.

Table 7: Metrics from the validation of the V2 snow cover product compared to the SMHI ground truth data. The accuracy, precision, recall and F1-score is presented for the validation.

Metric	V2
Accuracy	0.90
Precision	0.93
Recall	0.88
F1-Score	0.90

### 5.5 DATA AVAILABILITY OF V2 SNOW COVER PRODUCT

The results from the same method of cloud cover impact analysis that was done for the Sentinel-2 product are here presented for the V2 snow cover data. This aims to show the influence of cloud cover to the usability of the snow cover product has changed for the V2 product after the spatial fusion is used to combine IMS and Sentinel-2 data. Presented in Figure 17 is the percentage of data loss due to cloud cover for each month in the V2 dataset for all stations combined. The months of March, April and May show the most cloud cover in the V2 product compared to the rest of the year. These months saw the largest loss of usable data due to cloud cover. The lowest occurrence of clouds in the V2 product was in January.

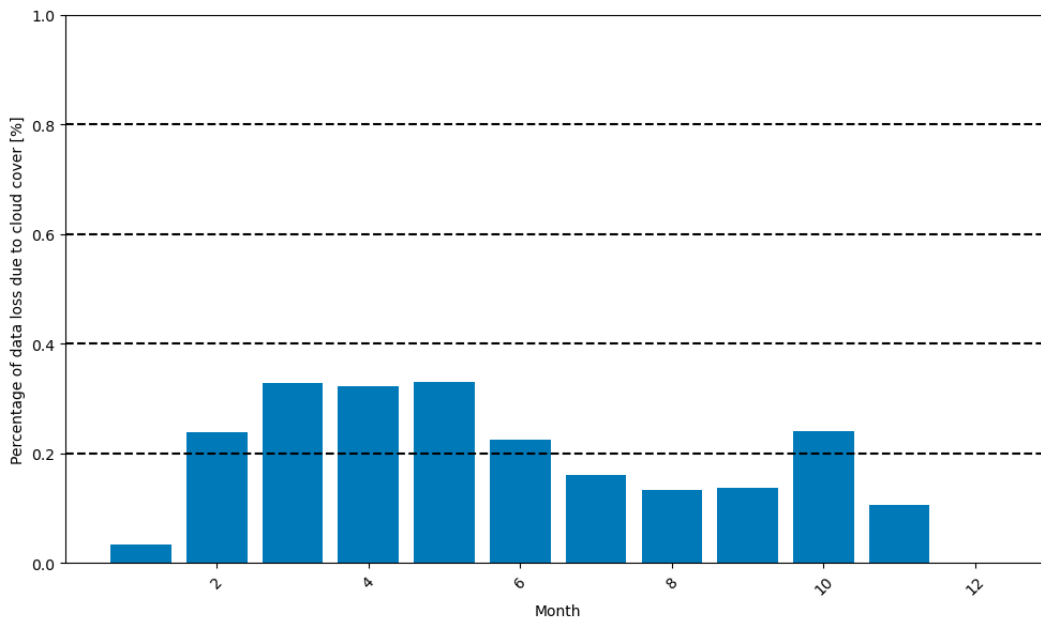


Figure 17: The percentage of data loss due to cloud cover for all stations, aggregated for each month in the V2 snow cover product.

In Figure 18 the yearly percentage of data loss due to cloud cover is presented for each station. Each color represents a different SMHI station. The pixelwise percentage of data loss due to cloud cover for the whole V2 dataset was 21.5%. This percentage considers all the pixels in the images and not only the pixels at the SMHI stations. When the gap limit was set to 5 days the pixelwise percentage of data loss due to cloud cover was 30.7%. The percentage of data loss due to cloud cover, both for the two days and the five days gap limit, was lower than the original 48.8% of Sentienl-2 FSC<sub>OG</sub> snow cover product for 2- and 5-days gap limit.

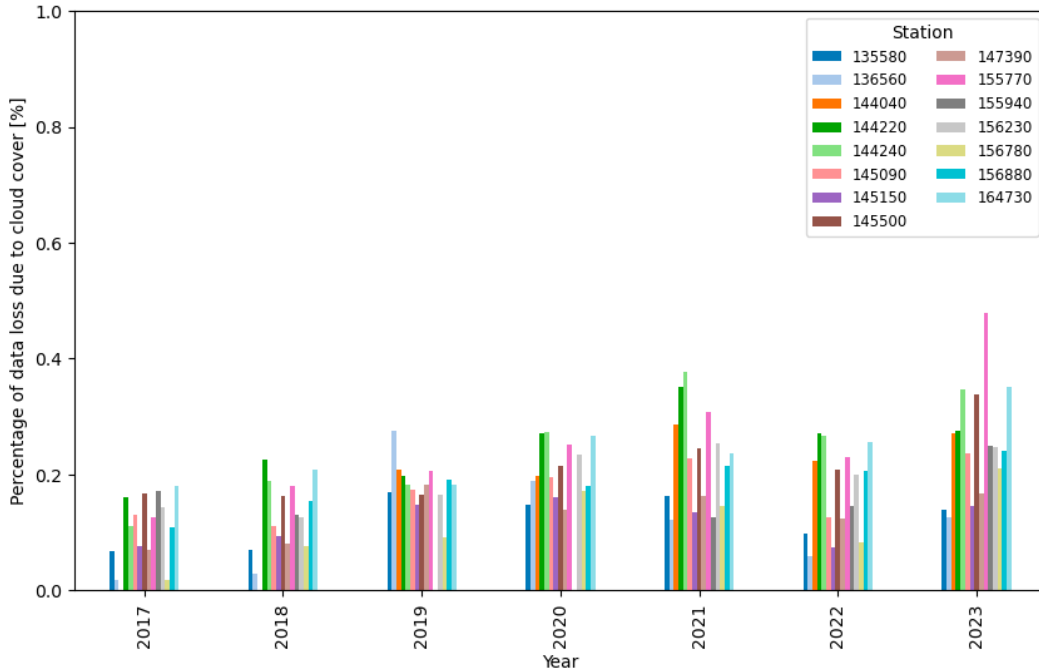


Figure 18: The percentage of data loss due to cloud cover at all stations for the V2 snow cover product. Each year is grouped together on the x-axis.

## 5.6 PART 2: SNOW COVER DYNAMICS

This section focuses on the snow cover dynamics observed during the validation of the V2 dataset from the spatiotemporal fusion. The analysis includes data from 10 stations (referred to as latitudes in this context), which is fewer than the 15 stations originally used for validation in this study. The SMHI stations 136560, 144040, 144220, 145090, and 155940 had substantial gaps in their snow data, making it impossible to accurately calculate snow dynamic metrics. Therefore, they were excluded from the analysis of snow cover dynamics.

Figure 19 illustrates the relationship between snow cover days and latitude. The snow cover days for each station (represented in the figure by their corresponding latitudes) are aggregated across all years and the average is presented here. The V2 data show higher snow cover days compared to the original FSC<sub>OG</sub> snow cover product. Higher amount of snow cover days is observed at higher latitudes. The average absolute difference between the V2 snow cover data and SMHI data were 12.8 days. This is a lower number compared to 19.4 days of the original Sentinel-2 FSC<sub>OG</sub> snow cover product but higher than the value of 7.4 for IMS.

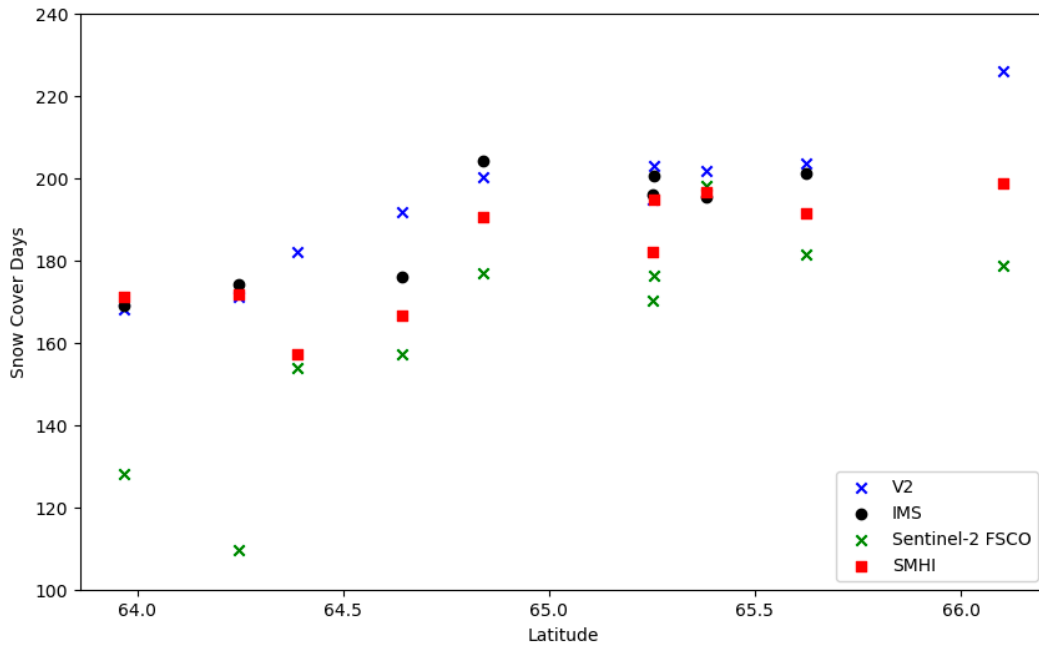


Figure 19: Comparison of snow cover days as a function of latitude for the V2 and Sentinel-2 FSCO<sub>OG</sub> snow cover products. Each year is aggregated for the stations and the mean is presented. On the x-axis is the SMHI station latitude. SMHI ground truth data in red, V2 in blue crosses, Sentinel-2 FSCO<sub>OG</sub> in green crosses and IMS in black.

The SCOD and SCED for the snow products and the SMHI data is presented in Figure 20. The hydrological year starts at the bottom of the y-axis. SMHI stations are here represented on the x-axis by their latitude. Longer snow seasons are observed for higher latitudes. The average absolute difference between the V2 data and SMHI data were 10.3 days. This is lower than the 21.1 days of the original Sentinel-2 FSCO<sub>OG</sub> snow cover product but higher than the value of 10.3 for IMS.

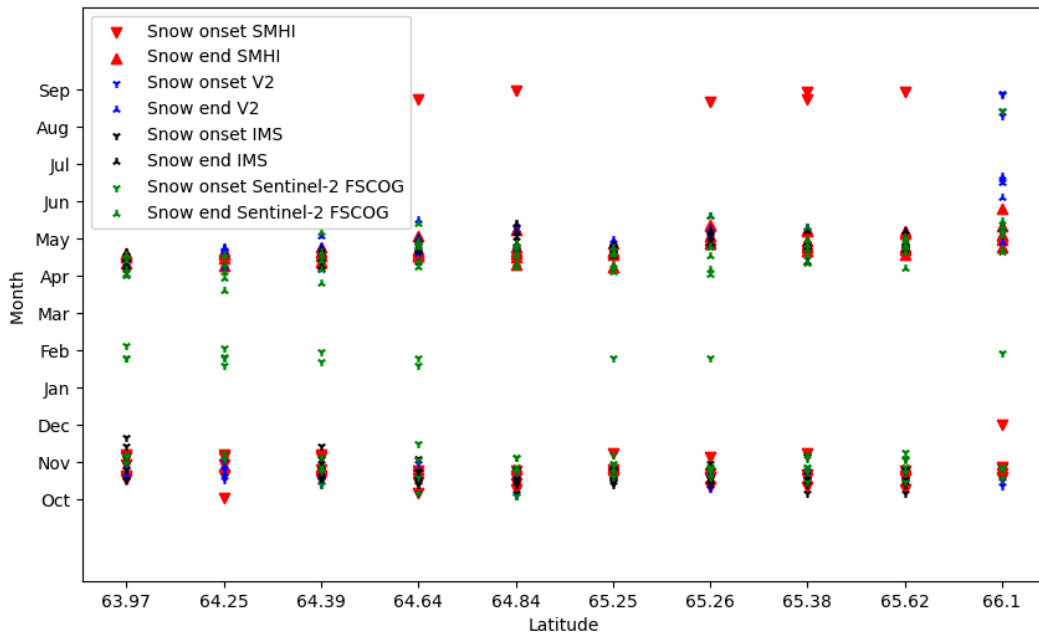


Figure 20: Snow onset and snow end dates for the V2 and original Sentinel-2 FSCO<sub>OG</sub> snow cover products and SMHI ground truth data. Onset is presented with downward-pointing markers, while end is presented with upward-pointing markers. On the x-axis is the SMHI station latitude. SMHI values in red, Sentinel-2 FSCO<sub>OG</sub> in green, V2 in blue and IMS in black.

## 5.7 PART 2: COMPARISON OF V2 SNOW COVER PRODUCT TO ORIGINAL SENTINEL-2 FSC<sub>OG</sub> AND IMS SNOW COVER PRODUCTS

This section presents examples of the new snow cover product from different dates and regions within the study area. Additionally, comparisons of the V2 snow cover product to the original Sentinel-2 FSC<sub>OG</sub> and IMS snow cover products are presented. An example of the difference mask use in the temporal fusion algorithm is also presented.

Figure 21 illustrates two Sentinel-2 FSC<sub>OG</sub> snow cover products to the left. They are from 10 and 13 May 2018. The region is the Sentinel-2 tile WWM. Snow is shown in grey, bare ground in black and clouds in white. The leftmost image that is from earlier in the snow season shows more snow compared to the middle one. The middle one that is from later in the snow season has more cloud cover. To the right is a result from the spatiotemporal fusion algorithm from the V2 dataset. It is based on the two Sentinel-2 FSC<sub>OG</sub> images and uses the difference mask presented in Figure 22 to fuse the images and create this image for 12 May 2018. It has the same amount of cloud cover as the leftmost image. The snow cover extent is less than the first image but larger than the second image.

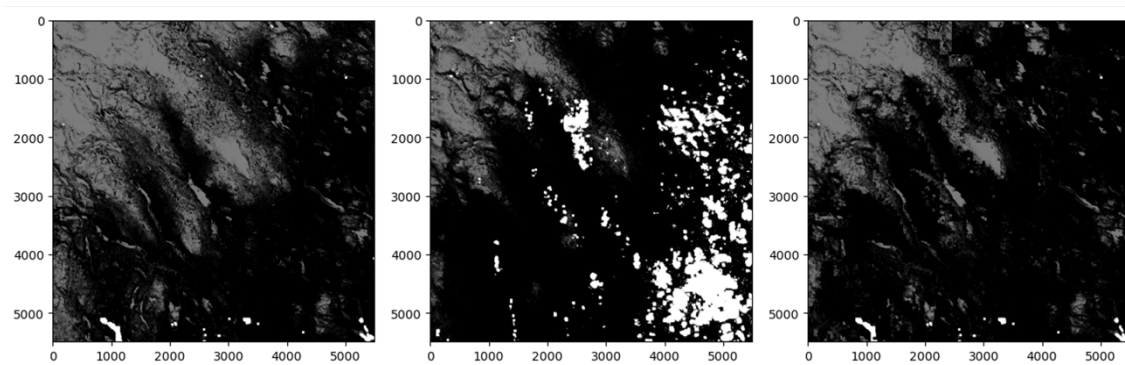


Figure 21: To the left and middle are two subsequent Sentinel-2 FSC<sub>OG</sub> from 10 May 2018 and 13 May 2018. The images have the extent of the Sentinel-2 tile id WWM. To the right is the resulting intermediate snow map in the V2 dataset from the fusion algorithm based on the two FSC<sub>OG</sub> images.

The temporal fusion algorithm uses the IMS images to detect the difference in the snowpack. This allows the subsequent Sentinel-2 FSC<sub>OG</sub> image to be projected on the previous one according to the detected change. Figure 22 shows two IMS images to the left. They cover the region of the Sentinel-2 tile WWM. The dates are 10 and 13 of May 2018. Snow is presented in white, waterbodies in grey and black is bare ground. The two IMS images show how the SCE decreases as the snow season comes to an end in the spring. To the right is the difference mask created from subtracting the two IMS images from each other. The white parts indicate where change is detected and black where no change occurred. The difference mask shows changes in the middle part of the image where there was snow in the first IMS image. No change is detected where both IMS images showed bare ground.

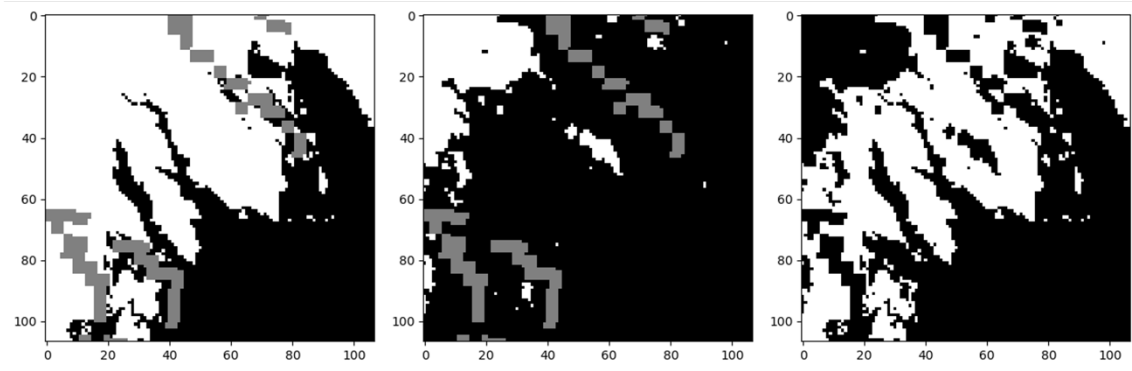


Figure 22: An example of how the difference mask is created from two IMS images. The images have the extent of the Sentinel-2 tile id WWM. To the left and middle are two following IMS acquisitions from 10 May 2018 and 13 May 2018. To the right is a difference mask created by subtracting the two IMS images.

## 6 DISCUSSIONS

The chapters 6.1 to 6.3 present a discussion of part 1 of the study. These were the results from the validation of the two snow cover products used in this study, Sentinel-2 FSC<sub>OG</sub> and IMS. The validation was conducted at each station in the SMHI data that was used as ground truth data. The stations were in the mountainous regions of Västerbotten and northern Jämtlands county. Snow cover dynamics of both the snow cover products were compared to the values derived from the SMHI ground truth data. An analysis of the cloud cover and data availability was conducted for the Sentinel-2 FSC<sub>OG</sub> snow cover product.

The chapters 6.4 to 6.7 present a discussion of part 2 of the study. These were the results from the validation of the V2 snow cover product created from the spatiotemporal fusion algorithm developed in this work. The validation was made with the same SMHI ground truth data as in part 1. The snow cover dynamics of the new V2 snow cover product was compared to the original Sentinel-2 FSC<sub>OG</sub> data and the ground truth data. The availability of V2 data and the cloud cover was also analyzed in a similar manner to that which was made to the Sentinel-2 FSC<sub>OG</sub> product. Examples of the V2 product are presented along with the IMS and Sentinel-2 FSC<sub>OG</sub> images used to create these examples.

These parts aim to discuss how the snow products performed in the mountainous regions of northern Sweden compared to the in situ measurements at the SMHI stations. The V2 product is the result of combining these through spatiotemporal fusion to extract the best aspects of each product. The discussion aims to address the opportunities and challenges that were discovered in the application of spatiotemporal fusion algorithms to these snow cover products.

### 6.1 PART 1: POINT BASED VALIDATION OF SENTINEL-2 AND IMS SNOW COVER PRODUCTS

The validation of the Sentinel-2 FSC<sub>OG</sub> and IMS snow cover products showed that they both had high accuracies of more than 90 % when evaluated on the SMHI ground truth station data as seen in Table 6. According to Table 5, IMS had more comparisons made due to the higher temporal resolution of the product. IMS is a daily product while Sentinel-2 FSC<sub>OG</sub> has a temporal resolution of 5-10 days (U.S. National Ice Center 2004, Copernicus Land Monitoring Service 2018). IMS show almost 10 times the number of comparisons made to the validation SMHI dataset than Sentinel-2 FSC<sub>OG</sub>. Despite the temporal resolution not being 10 times better. This can be a result of the polar night at these latitudes (Dietz et al. 2012b) that leads to insufficient illumination for Sentinel-2 FSC<sub>OG</sub>. The differences in temporal and spatial resolution are important to consider when comparing the accuracy of the two snow cover products. Different applications in monitoring of snow cover dynamics have different requirements of spatial and temporal resolution. SCD can benefit from higher spatial distribution if the snow cover is highly heterogenous. SCOD and SCED might on the other hand need high temporal resolution to detect rapid changes in the start and end of the snow season not to miss the day when snow cover starts or ends.

To compare the snow cover products performances with a confusion matrix the normalized confusion matrix in Figure 9 is more suitable than the absolute numbers from the unnormalized confusion matrix. IMS had higher accuracies for TP with 97% compared to 94% of Sentinel-2 FSC<sub>OG</sub>. IMS therefore more seldomly miss detecting snow cover. Sentinel-2 FSC<sub>OG</sub> on the other hand had better TN of 97% compared to 89% of IMS and are thus better at detecting when no snow is present. This is reasonable since snow and no snow

cover are the opposites of each other. Sentinel-2 FSC<sub>OG</sub> have higher FN since it tends to underestimate SCE. This is also illustrated in Table 6. Sentinel-2 FSC<sub>OG</sub> had higher precision than recall, which means that while a greater portion of its positive snow cover classifications are correct, it misses some of the instances when snow was present. In contrast, IMS had lower precision than recall which indicates that it is less likely to miss snow cover but sometimes classifies bare ground as snow covered. This agrees with the findings that the creators of the LIS algorithm for the Sentinel-2 FSC<sub>OG</sub> product found of it underestimating snow detection. The authors used a similar approach of validation with data from snow stations (Gascoin et al. 2019).

When assessing the total performance of the two snow cover products, the F1-score is a good indication since it weights both the recall and precision into a harmonic weighted mean. Sentinel-2 FSC<sub>OG</sub> had a higher F1-score compared to IMS if only slightly higher indicating a better overall snow cover product. This was valid for the comparison on the SMHI station data.

The IMS snow cover product is produced with information from in situ measurements in some instances. Information about when this happens is not available. This is an issue since the possibility of validating the IMS product on the same in situ data as it was produced from can't be ensured. This method of validating the IMS product on in situ measurements has been performed previously (Chen et al. 2012) and this study found similar accuracy as previous studies have found between 85-95% (Helfrich et al. 2018). It is still possible that these measurements are biased when the in situ measurements are used to produce the IMS product. In further studies it would be recommended to further examine the possibilities of obtaining information about when and which in situ measurements are used for the IMS product.

## **6.2 PART 1: CLOUD IMPACT ANALYSIS OF SENTINEL-2 FSC<sub>OG</sub> SNOW COVER PRODUCT**

Since the Sentinel-2 FSC<sub>OG</sub> snow cover product is based on remote sensed data in the visible part of the spectrum the product is hindered by cloud cover and insufficient illumination due to the sun incident angle (HR-S&I 2023). Figure 8 shows that in the winter months there are very few acquisitions for the Sentinel-2 snow cover product that can be a result of the low illumination during winter. This highlights the problem with using optical sensors for snow cover mapping. The cloud impact analysis was conducted to quantify the extent of the problem with cloud cover and its influence on the availability of snow cover data in the Sentinel-2 FSC<sub>OG</sub> snow cover product. The IMS dataset was not analyzed for impact of cloud cover since it uses multiple sources such as microwave that can penetrate clouds. No cloud coverage are therefore present in the IMS snow cover dataset (U.S. National Ice Center 2004).

Cloud cover was present in the FSC<sub>OG</sub> product around 40% of the times that the product was compared to the values at the SMHI stations as seen in Figure 10. A seasonal pattern of less clouds during the summer months compared to the winter is observed in the analysis. This is a pattern observed by Dietz et al. (2012b) for the MODIS snow cover data. The distribution of FSC<sub>OG</sub> acquisitions throughout the year varies greatly as observed in Figure 11. This might lead to inaccurate estimations of cloud cover for the months January and December since very few or no acquisitions were made in those months. Figure 10 also highlights the problem that polar darkness poses on snow cover mapping in high latitude regions. The absence of acquisitions in December and January are caused by insufficient sunlight during those months. This is also observed in the MODIS snow cover product by Dietz et al. (2012b).

In 2021 the stations 144220 and 144240 had higher percentage of data impacted by clouds than the other stations as seen in Figure 11. For those stations around 70% unusable data due to cloud cover was observed for 2021, leading to very little usable snow cover data. Station 136560 saw 100% unusable data due to cloud cover in the FSC<sub>OG</sub> acquisitions from 2017. The year of 2017 only had one acquisition for over the station 136560 which was obscured by clouds resulting in the 100% cloud cover. From Figure 12 it was found that the cloud cover in the study varies with longitude and not with latitude. To validate this an additional analysis which includes elevation data for the stations would be needed. The western regions of the study area are more mountainous which can explain the trend seen for longitude. The land cover type is similar along a latitudinal path in the study area. This combined with the relatively short latitudinal difference of only 2 degrees can explain why there is no trend in cloud cover with latitude.

For the whole dataset at every pixel, clouds were present 48.8% of the time which is close to the 46.8% that Dietz et al. (2012b) found for the MODIS snow cover product over the whole of Europe. A more extensive study for the pixelwise cloud cover distribution over the seasons would be useful to fully evaluate the impact of cloud cover in the FSC<sub>OG</sub> product. That was not done in this study due to time constraints.

### **6.3 PART 1: SNOW COVER DYNAMICS OF SENTINEL-2 FSC<sub>OG</sub> AND IMS SNOW COVER PRODUCTS**

The snow cover dynamics calculated from both the snow cover products show similar results of those observed in the validation in section 6.1. Figure 13 illustrates how IMS overestimates the SCD and FSC<sub>OG</sub> underestimates SCD compared to SMHI ground truth data. The forward fill method used to extend the FSC<sub>OG</sub> snow cover product only extends the current snow cover state until a new acquisition is available. This is a very inaccurate interpolation since it does not use any input as how the snow state changes between acquisitions. FSC<sub>OG</sub> have more than double the difference in SCD compared to SMHI than IMS, 19.4 and 7.4 days on average for the snow products. This speaks for the temporal resolution being a more important factor in determining SCD. Therefore, achieving better results for IMS and combining the two products to improve snow cover dynamics measurements, as suggested by Rittger et al. (2021), is the reason behind their work.

The disadvantages of the low temporal resolution and the effect of polar darkness for FSC<sub>OG</sub> are illustrated in Figure 14. For several of the stations and snow seasons examined the SCOD is in February or January. This is far off from the actual SCOD from SMHI data in November. The low temporal resolution and high ratios of cloud cover can result in no snow cover being detected before the polar darkness. This appears to be more common at lower latitudes where the SCOD occurs later in the year. That can be the reason for the large error in SCOD and SCED for FSC<sub>OG</sub> compared to SMHI data. The difference in SCOD and SCED compared to the SMHI data was more than twice the length for FSC<sub>OG</sub> than IMS, 21.1 and 10.3 days on average.

IMS coarse spatial resolution is the reason why there are only 8 SCOD and SCED calculated compared to 10 for the FSC<sub>OG</sub> product. As some stations lie close to waterbodies they are consistently incorrectly classified as ice or water. The FSC<sub>OG</sub> product don't have this problem since it has higher spatial resolution and can therefore detect snow closer to water. This emphasizes the need of higher spatial resolution in some applications.

#### **6.4 PART 2: POINT BASED VALIDATION OF V2 SNOW COVER PRODUCT**

One advantage of the V2 product compared to the FSC<sub>OG</sub> product are the total number of comparisons made to the SMHI ground truth data. This is because of the daily temporal resolution that the spatiotemporal fusion algorithm can achieve by utilizing the favorable temporal attributes of the IMS dataset. In total 26 809 comparisons were made compared to the 1 730 of the FSC<sub>OG</sub> product as shown in Figure 16 and Table 5. This benefits most applications acquiring snow cover maps since it gives more frequently updated data and can in turn result in more accurate hydrological models (Dong 2018).

Figure 16 and Table 7 shows that the accuracy for the v2 product is lower than that of the original snow cover products. The V2 products tends to underestimate like the FSC<sub>OG</sub> product, showing the characteristics being carried over from the product in the fusion. The higher spatial resolution of the V2 must be considered when assessing the overall performance. For snow cover classification in areas that have high spatial variability it can be beneficial to have snow maps with high spatial resolution to capture the variations due to wind drift for example (Mott et al. 2018). The accuracy of the V2 product can be inferior because of the effect that the water mask in IMS has. The fusion algorithm does not consider waterbodies in the IMS product and can therefore include water or ice in the new V2 product when the gap limit is surpassed. This was done since FSC<sub>OG</sub> doesn't have values for water. The individual confusion matrixes for V2 in Appendix 9.1.3 show that some stations have very low TP scores. These stations are the ones excluded from the validation of the IMS product because of consistent classification as water. This could not be done for the V2 product since it doesn't have a value for water. An improvement to the spatiotemporal fusion algorithm presented in this work could be to add a way of removing IMS water or ice pixels in the fusion so they are not included in the V2 product.

#### **6.5 PART 2: DATA AVAILABILITY OF V2 SNOW COVER PRODUCT**

The data availability analysis showed that the V2 product has more snow cover data available. This is the result of combining the high temporal properties of the IMS dataset. Doing this creates a dataset which allows for continuous monitoring of the snowpack. The difference is especially noticeable during the mid-winter months when there also is polar darkness. This can be because of the gap limit in the algorithm being exceeded and IMS is instead used exclusively during this period. These months then don't achieve the high spatial resolution that the FSC<sub>OG</sub> product contributes with during the rest of the year. As the gap limit is increased the total pixelwise frequency of cloud presence goes from 21.5% for the V2 dataset to 30.7% for 5-day gap limit. The properties of the product from the fusion algorithm are similar to the FSC<sub>OG</sub> product when the gap limit is increased since there are less days when the IMS data is used. With an infinite gap limit the product from the fusion algorithm won't have any IMS data in it.

When looking at individual stations in Figure 18 the impact of cloud cover is also less compared to the original FSC<sub>OG</sub> product. There is also seasonal variation between the years that are reflected in more cloud cover for example in 2021. This shows that reducing the effect of cloud cover can be especially important in some seasons when cloud cover is especially high. The distribution of available data is more consistent than the FSC<sub>OG</sub> product. Figure 15 shows that each month has around 8% of the available data in the V2 snow cover product. The inclusion of the IMS product contributes to filling in the data gaps for the months where the FSC<sub>OG</sub> has no data because of polar night. That is the benefit of the passive microwave sensors that IMS uses to detect snow cover (Helfrich et al. 2018). This has previously been seen as a key benefit of using passive microwave remote sensing for snow

cover mapping (Dietz et al. 2012a; Dong 2018). Here it is utilized in combination with the high spatial resolution of optical sensors to mitigate the negative impact of cloud cover. This has been previously proposed for general spatiotemporal fusion algorithms not specifically focusing on snow cover mapping by Belgiu & Stein (2019).

## **6.6 PART 2: SNOW COVER DYNAMICS OF V2 SNOW COVER PRODUCT**

The V2 snow cover product saw improvements in characterizing both snow season duration (SCOD and SCED) and SCD compared to the high-resolution Sentinel-2 snow cover product. Figure 19 shows that the V2 product generally overestimated the SCD compared to the SMHI ground truth data. It shows similar characteristics to the those of the SCD for the IMS product. The difference to the SMHI data was reduced by 6.6 days to 12.8 days approaching the value of the IMS product of 7.4 days. This shows the benefit of fusing the high temporal resolution IMS product with the  $FSC_{OG}$  product. SCD need continuous data to accurately detect rapid changes in snow accumulation and snow melting which occurs during periods outside of the polar night. During the polar night it is more important to have sensors that are capable to gather data regardless of how much light is present. Similar to the approach by Esmaelzadeh et al. (2024), which integrates cloud-penetrating Sentinel-1 data with optical Sentinel-2 images for more accurate snow water content mapping, this study's method combines different products. This combination aims to achieve enhanced results in measuring snow cover dynamics in a comparable manner.

The SCOD and SCED was improved compared to the original  $FSC_{OG}$  product as seen in Figure 20. The difference to the SMHI data was 10.3 days which is the same as the IMS data. Important to note is that V2 achieved this accuracy while having a snow cover data of higher spatial resolution on days in proximity to  $FSC_{OG}$  data, that will say within the gap limit in the fusion algorithm set by the user. The V2 product did not have the same problem as  $FSC_{OG}$  had with SCOD in January and February. By using the IMS data there were no gaps long enough in the data that resulted in missing the start of the snow season.

The spatiotemporal fusion algorithm succeeds in achieving better results in the snow cover dynamics measured in this study. A higher temporal and spatial resolution than the individual snow cover products were also attained for the V2 data. This indicates that spatiotemporal fusion of optical and microwave-based snow cover products is suitable for improving snow cover mapping.

## **6.7 PART 2: COMPARISON OF V2 SNOW COVER PRODUCT TO ORIGINAL SENTINEL-2 $FSC_{OG}$ AND IMS SNOW COVER PRODUCTS**

The example from the spatiotemporal fusion in Figure 21 show how two Sentinel-2  $FSC_{OG}$  images are fused to create the V2 product. The scenes are from the peak of snow melt season when big changes occur in the distribution of the snowpack. This time was chosen to illustrate clearly what happens in the algorithm. During mid-winter the snowpack is consistent and no changes in SCE occur. The new V2 product is a fusion of the two  $FSC_{OG}$  products as mentioned before, this can be seen in different parts of the picture. The difference mask shown in Figure 22 indicates where the change in the snowpack between the two dates occurred. These parts are therefore retrieved from the second  $FSC_{OG}$  image. Where now change occurred are retrieved from the first  $FSC_{OG}$  image.

The algorithm makes a good job of not copying cloud cover in the fusion process. The clouds in the second  $FSC_{OG}$  image are not copied in the fusion since the algorithm filters out those. In the case where clouds are present in both the  $FSC_{OG}$  images no information about the

snowpack exists for any of the images and cloud can't be filtered out. An improvement might be made in the algorithm to use the IMS data for these pixels when this happens. That can also be made for images with no-data pixels. Some of the FSC<sub>OG</sub> tiles have areas of no-data because of the acquisition path of the Sentinel-2 satellite. Utilizing the IMS data in these cases could increase the available snow cover data for the V2 product.

With interval between the two acquisitions being 3 days there can be weather events that have happened that we do not see in the FSC<sub>OG</sub> images. If snow had fallen on one of the days and melted before the new FSC<sub>OG</sub> image the V2 image between the two FSC<sub>OG</sub> images will not be able to reflect that. That is why the gap limit was introduced in the algorithm to control how long of a gap between FSC<sub>OG</sub> acquisitions is tolerated. Too long of a gap increases the risk of missing changes in the snow cover from melting or new snow fall. This could be mitigated by having the difference mask from the IMS data track if the difference is positive (snow cover increased) or negative (snow cover melted). Currently the difference mask only tracks if a change occurred and not the type of change.

## 7 CONCLUSIONS

The results from the validation of the snow cover products Sentinel-2 FSC<sub>OG</sub> and IMS show that both products have high accuracies with more than 90% percent correct classifications when compared to the ground truth data SMHI consisting of in situ measurements. IMS had higher recall meaning that it was less likely to miss snow cover compared to Sentinel-2 FSC<sub>OG</sub>. On the other hand, Sentinel-2 FSC<sub>OG</sub> was more accurate at predicting bare ground, avoiding false positives when no snow was present. Sentinel-2 FSC<sub>OG</sub> therefore tends to underestimate the snow cover whilst IMS tends to overestimate the snow cover. This difference is important to consider when using the snow cover products for applications like hydrological modelling and analysis of snow cover dynamics.

The analysis of the cloud cover showed that about 40% the data from the Sentinel-2 FSC<sub>OG</sub> snow cover product was unusable because of cloud cover. A seasonal variation with the winter months having more cloud cover was observed. Additionally the western and more mountainous parts had more cloud cover. This limits the availability of the snow cover data of the already low temporal resolution Sentinel-2 FSC<sub>OG</sub> snow cover product.

Through a spatiotemporal fusion algorithm of the two snow cover products a new dataset was generated named V2. The purpose of the spatiotemporal fusion was to combine the best attributes of each dataset, the high temporal resolution of IMS and the high spatial resolution of Sentinel-2 FSC<sub>OG</sub>. As a result of the spatiotemporal fusion algorithm the V2 product has a daily temporal resolution and maintained the high spatial resolution from the FSC<sub>OG</sub> product. The results from the data availability analysis of the V2 product showed a reduction of cloud pixels with 21.5% cloud cover with a gap limit of 2 days and 30.7% with a gap limit of 5 days. This shows a higher temporal resolution and a reduction of unusable data allowing continuous monitoring of the snow cover at high spatial resolution.

The snow cover dynamics from the V2 product showed improvements in the studied metrics snow cover days, snow cover onset and snow cover end day compared to the original Sentinel-2 FSC<sub>OG</sub> product. The new V2 product did not surpass the IMS product in the studied snow cover metrics. The average difference in snow cover days between the V2 and SMHI data was 12.8 days which is an improvement to the 19.4 days of the Sentinel-2 FSC<sub>OG</sub> product and closer to the 7.4 days of the IMS product. For the SCOD and SCED the difference between the V2 and SMHI data was 10.3 days, the same as the IMS product and an improvement compared to the 21.1 days of Sentinel-2 FSC<sub>OG</sub>. This suggests that combining the optical Sentinel-2 FSC<sub>OG</sub> snow cover product with the IMS snow cover product, which uses passive microwave and other sources, through spatiotemporal fusion could enhance snow cover mapping. This approach can be useful when improved temporal and spatial resolution can be prioritized over accuracy.

## 8 REFERENCES

- Andreadis, K.M. & Lettenmaier, D.P. (2006). Assimilating remotely sensed snow observations into a macroscale hydrology model. *Advances in Water Resources*, 29 (6), 872–886. <https://doi.org/10.1016/j.advwatres.2005.08.004>
- Barnett, T.P., Adam, J.C. & Lettenmaier, D.P. (2005). Potential impacts of a warming climate on water availability in snow-dominated regions. *Nature*, 438 (7066), 303–309. <https://doi.org/10.1038/nature04141>
- Belgiu, M. & Stein, A. (2019). Spatiotemporal Image Fusion in Remote Sensing. *Remote Sensing*, 11 (7), 818. <https://doi.org/10.3390/rs11070818>
- Bormann, K.J., Brown, R.D., Derksen, C. & Painter, T.H. (2018). Estimating snow-cover trends from space. *Nature Climate Change*, 8 (11), 924–928. <https://doi.org/10.1038/s41558-018-0318-3>
- Box, G.E.P. (1979). Robustness in the Strategy of Scientific Model Building. I: Launer, R.L. & Wilkinson, G.N. (red.) *Robustness in Statistics*. Academic Press. 201–236. <https://doi.org/10.1016/B978-0-12-438150-6.50018-2>
- CGLS (2024a). *Snow Cover Extent*. Copernicus Global Land Service (CGLS). <https://land.copernicus.eu/global/products/sce> [2024-02-20]
- CGLS (2024b). *Snow Water Equivalent*. Copernicus Global Land Service (CGLS). <https://land.copernicus.eu/global/products/swe> [2024-02-16]
- Chen, C., Lakhankar, T., Romanov, P., Helfrich, S., Powell, A. & Khanbilvardi, R. (2012). Validation of NOAA-Interactive Multisensor Snow and Ice Mapping System (IMS) by Comparison with Ground-Based Measurements over Continental United States. *Remote Sensing*, 4 (5), 1134–1145. <https://doi.org/10.3390/rs4051134>
- Copernicus Land Monitoring Service (2018). COSIMS-DT-060-MAG\_PUM\_SNOW\_3.6. (3)
- Dietz, A.J., Kuenzer, C., Gessner, U. & Dech, S. (2012a). Remote sensing of snow – a review of available methods. *International Journal of Remote Sensing*, 33 (13), 4094–4134. <https://doi.org/10.1080/01431161.2011.640964>
- Dietz, A.J., Wohner, C. & Kuenzer, C. (2012b). European Snow Cover Characteristics between 2000 and 2011 Derived from Improved MODIS Daily Snow Cover Products. *Remote Sensing*, 4 (8), 2432–2454. <https://doi.org/10.3390/rs4082432>
- Dong, C. (2018). Remote sensing, hydrological modeling and in situ observations in snow cover research: A review. *Journal of Hydrology*, 561, 573–583. <https://doi.org/10.1016/j.jhydrol.2018.04.027>
- Dozier, J. (1989). Spectral signature of alpine snow cover from the Landsat Thematic Mapper. *Remote Sensing of Environment*, 28. [https://doi.org/10.1016/0034-4257\(89\)90101-6](https://doi.org/10.1016/0034-4257(89)90101-6)
- Earth Science Data Systems, N. (2024). *What is Remote Sensing?* | *Earthdata*. [Background]. <https://www.earthdata.nasa.gov/learn/backgrounders/remote-sensing> [2024-

03-05]

Esmaelzadeh, R., Emamgholizadeh, S. & Bigdeli, B. (2024). Improvement on the Effective Snow Cover Extraction Using Fusion Satellite Images Approach. *Journal of the Indian Society of Remote Sensing*, 52 (2), 449–462. <https://doi.org/10.1007/s12524-024-01828-y>

European Space Agency (2024). *Sentinel-2 - Missions - Sentinel Online*. *Sentinel Online*. <https://copernicus.eu/missions/sentinel-2> [2024-03-14]

Flanner, M.G., Shell, K.M., Barlage, M., Perovich, D.K. & Tschudi, M.A. (2011). Radiative forcing and albedo feedback from the Northern Hemisphere cryosphere between 1979 and 2008. *Nature Geoscience*, 4 (3), 151–155. <https://doi.org/10.1038/ngeo1062>

Gafurov, A. & Bárdossy, A. (2009). Cloud removal methodology from MODIS snow cover product. *Hydrology and Earth System Sciences*, 13 (7), 1361–1373. <https://doi.org/10.5194/hess-13-1361-2009>

Gascoin, S., Grizonnet, M., Bouchet, M., Salgues, G. & Hagolle, O. (2019). Theia Snow collection: high-resolution operational snow cover maps from Sentinel-2 and Landsat-8 data. *Earth System Science Data*, 11 (2), 493–514. <https://doi.org/10.5194/essd-11-493-2019>

Hall, D.K. & Riggs, G.A. (2010). Normalized-Difference Snow Index (NDSI). <https://ntrs.nasa.gov/citations/20100031195> [2024-02-08]

Hall, D.K., Riggs, G.A. & Salomonson, V.V. (1995). Development of methods for mapping global snow cover using moderate resolution imaging spectroradiometer data. *Remote Sensing of Environment*, 54 (2), 127–140. [https://doi.org/10.1016/0034-4257\(95\)00137-P](https://doi.org/10.1016/0034-4257(95)00137-P)

Hall, D.K., Riggs, G.A., Salomonson, V.V., DiGirolamo, N.E. & Bayr, K.J. (2002). MODIS snow-cover products. *Remote Sensing of Environment*, 83 (1–2), 181–194. [https://doi.org/10.1016/S0034-4257\(02\)00095-0](https://doi.org/10.1016/S0034-4257(02)00095-0)

Hardin, P. & Shumway, J.M. (1997). Statistical significance and normalized confusion matrices. *Photogrammetric Engineering and Remote Sensing*, 63

Hecheltjen, A., Thonfeld, F. & Menz, G. (2014). Recent Advances in Remote Sensing Change Detection – A Review. I: Manakos, I. & Braun, M. (red.) *Land Use and Land Cover Mapping in Europe: Practices & Trends*. Springer Netherlands. 145–178. [https://doi.org/10.1007/978-94-007-7969-3\\_10](https://doi.org/10.1007/978-94-007-7969-3_10)

Helfrich, S., Li, M., Kongoli, C., Nagdimunov, L. & Rodriguez, E. (2018). IMS ALGORITHM THEORETICAL BASIS DOCUMENT VERSION 2.4.

HR-S&I (2023). *ALGORITHM THEORETICAL BASIS DOCUMENT FOR SNOW PRODUCTS BASED ON SENTINEL-2*. (COSIMS-DT-062-MAG\_ATBD\_SNOW). <https://land.copernicus.eu/en/technical-library/hrsi-snow-atbd/@@download/file> [2024-01-30]

Jylhä, K., Fronzek, S., Tuomenvirta, H., Carter, T.R. & Ruosteenoja, K. (2008). Changes in frost, snow and Baltic sea ice by the end of the twenty-first century based on climate model projections for Europe. *Climatic Change*, 86 (3), 441–462. <https://doi.org/10.1007/s10584-007-9310-z>

- Klein, A.G. & Barnett, A.C. (2003). Validation of daily MODIS snow cover maps of the Upper Rio Grande River Basin for the 2000–2001 snow year. *Remote Sensing of Environment*, 86 (2), 162–176. [https://doi.org/10.1016/S0034-4257\(03\)00097-X](https://doi.org/10.1016/S0034-4257(03)00097-X)
- Klein, G., Vitasse, Y., Rixen, C., Marty, C. & Rebetez, M. (2016). Shorter snow cover duration since 1970 in the Swiss Alps due to earlier snowmelt more than to later snow onset. *Climatic Change*, 139 (3), 637–649. <https://doi.org/10.1007/s10584-016-1806-y>
- Kulkarni, A., Chong, D. & Batarseh, F.A. (2020). 5 - Foundations of data imbalance and solutions for a data democracy. I: Batarseh, F.A. & Yang, R. (red.) *Data Democracy*. Academic Press. 83–106. <https://doi.org/10.1016/B978-0-12-818366-3.00005-8>
- Largeron, C., Dumont, M., Morin, S., Boone, A., Lafaysse, M., Metref, S., Cosme, E., Jonas, T., Winstral, A. & Margulis, S.A. (2020a). Toward Snow Cover Estimation in Mountainous Areas Using Modern Data Assimilation Methods: A Review. *Frontiers in Earth Science*, 6, 81–94
- Largeron, C., Dumont, M., Morin, S., Boone, A., Lafaysse, M., Metref, S., Cosme, E., Jonas, T., Winstral, A. & Margulis, S.A. (2020b). Toward Snow Cover Estimation in Mountainous Areas Using Modern Data Assimilation Methods: A Review. *Frontiers in Earth Science*, 8. <https://www.frontiersin.org/articles/10.3389/feart.2020.00325> [2024-02-15]
- Liang, S. & Wang, J. (red.) (2020). Chapter 1 - A systematic view of remote sensing. I: *Advanced Remote Sensing (Second Edition)*. Academic Press. 1–57. <https://doi.org/10.1016/B978-0-12-815826-5.00001-5>
- Mott, R., Vionnet, V. & Grünwald, T. (2018). The Seasonal Snow Cover Dynamics: Review on Wind-Driven Coupling Processes. *Frontiers in Earth Science*, 6. <https://www.frontiersin.org/articles/10.3389/feart.2018.00197> [2024-02-15]
- Naturvårdsverket (2023). National Land Cover Database (NMD). <https://www.naturvardsverket.se/en/services-and-permits/maps-and-map-services/national-land-cover-database/> [2024-02-18]
- Parajka, J. & Blöschl, G. (2008). Spatio-temporal combination of MODIS images – potential for snow cover mapping. *Water Resources Research*, 44 (3). <https://doi.org/10.1029/2007WR006204>
- Penn State (u.å.). *Observing Weather from Space | Learning Weather at Penn State Meteorology*. <https://learningweather.psu.edu/node/46> [2024-07-13]
- Pohl, C. & Van Genderen, J.L. (1998). Review article Multisensor image fusion in remote sensing: Concepts, methods and applications. *International Journal of Remote Sensing*, 19 (5), 823–854. <https://doi.org/10.1080/014311698215748>
- Read, J.M. & Torrado, M. (2009). Remote Sensing. I: Kitchin, R. & Thrift, N. (red.) *International Encyclopedia of Human Geography*. Elsevier. 335–346. <https://doi.org/10.1016/B978-008044910-4.00508-3>
- Revuelto, J., Alonso-González, E., Gascoin, S., Rodríguez-López, G. & López-Moreno, J.I. (2021). Spatial Downscaling of MODIS Snow Cover Observations Using Sentinel-2 Snow Products. *Remote Sensing*, 13 (22), 4513. <https://doi.org/10.3390/rs13224513>

- Rittger, K., Krock, M., Kleiber, W., Bair, E.H., Brodzik, M.J., Stephenson, T.R., Rajagopalan, B., Bormann, K.J. & Painter, T.H. (2021). Multi-sensor fusion using random forests for daily fractional snow cover at 30 m. *Remote Sensing of Environment*, 264, 112608. <https://doi.org/10.1016/j.rse.2021.112608>
- Salomonson, V.V. & Appel, I. (2004). Estimating fractional snow cover from MODIS using the normalized difference snow index. *Remote Sensing of Environment*, 89 (3), 351–360. <https://doi.org/10.1016/j.rse.2003.10.016>
- SMHI (2024). *Snö* | *SMHI*. <https://www.smhi.se/data/meteorologi/sno> [2024-03-08]
- U.S. National Ice Center (2004). IMS Daily Northern Hemisphere Snow and Ice Analysis at 1 km, 4 km, and 24 km Resolutions, Version 1. <https://doi.org/10.7265/N52R3PMC>
- U.S. National Ice Center. (2008). IMS Daily Northern Hemisphere Snow and Ice Analysis at 1 km, 4 km, and 24 km Resolutions, Version 1 [Data set]. <https://doi.org/10.7265/N52R3PMC>
- Wang, X., Xie, H. & Liang, T. (2008). Evaluation of MODIS snow cover and cloud mask and its application in Northern Xinjiang, China. *Remote Sensing of Environment*, 112 (4), 1497–1513. <https://doi.org/10.1016/j.rse.2007.05.016>
- Zhang, J., Pohjola, V.A., Pettersson, R., Norell, B., Marchand, W.-D., Clemenzi, I. & Gustafsson, D. (2021). Improving the snowpack monitoring in the mountainous areas of Sweden from space: a machine learning approach. *Environmental Research Letters*, 16 (8), 084007. <https://doi.org/10.1088/1748-9326/abfe8d>
- Zhu, X., Cai, F., Tian, J. & Williams, T.K.-A. (2018). Spatiotemporal Fusion of Multisource Remote Sensing Data: Literature Survey, Taxonomy, Principles, Applications, and Future Directions. *Remote Sensing*, 10 (4), 527. <https://doi.org/10.3390/rs10040527>

## 9 APPENDIX

### 9.1 INDIVIDUAL STATION SNOW COVER PRODUCT CONFUSION MATRIX

#### 9.1.1 FSC<sub>OG</sub>

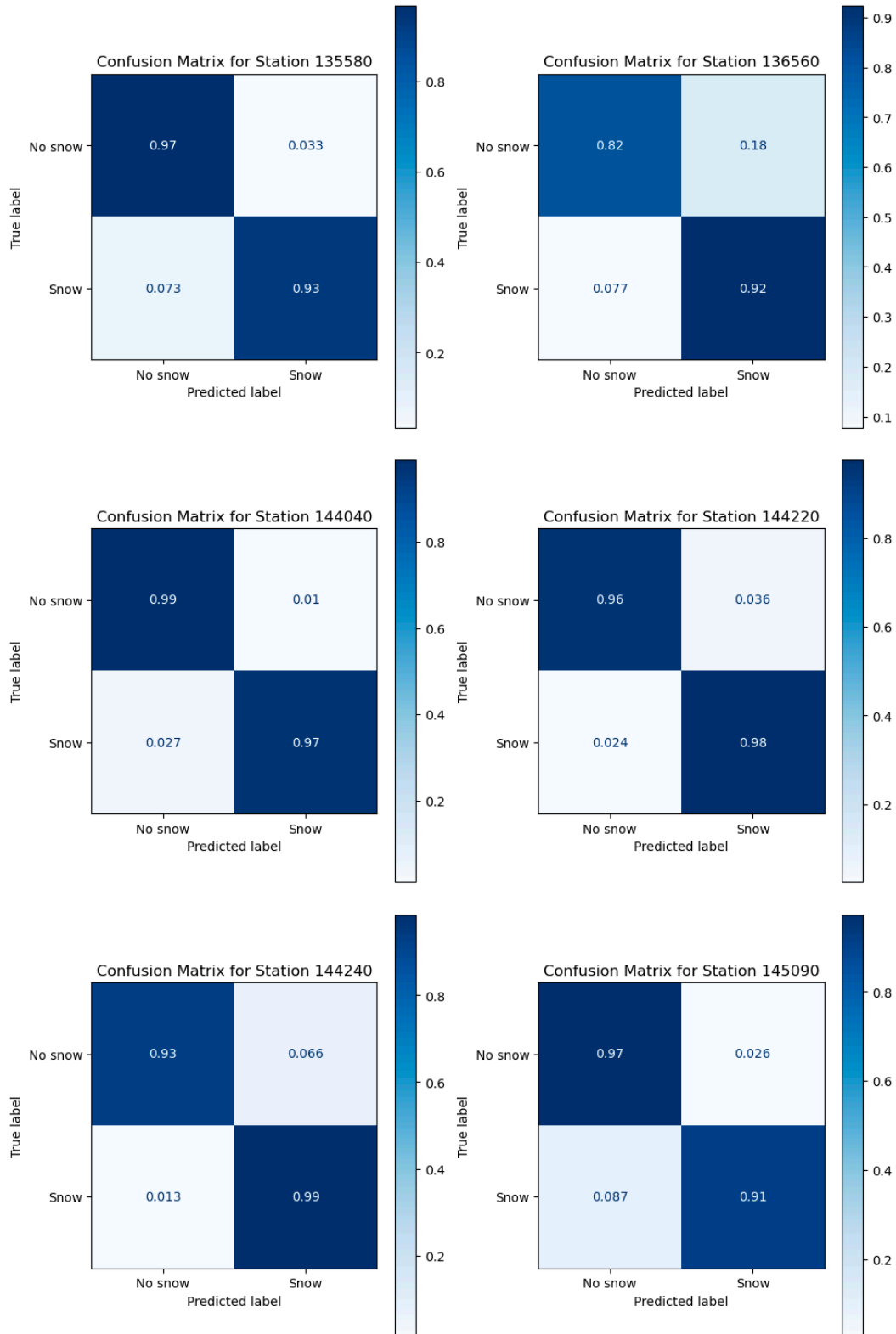


Figure 23: Confusion matrix of Sentinel-2 FSC<sub>OG</sub> snow product for individual stations evaluated on SMHI ground truth data. Values normalized by number of acquisitions per snow product.

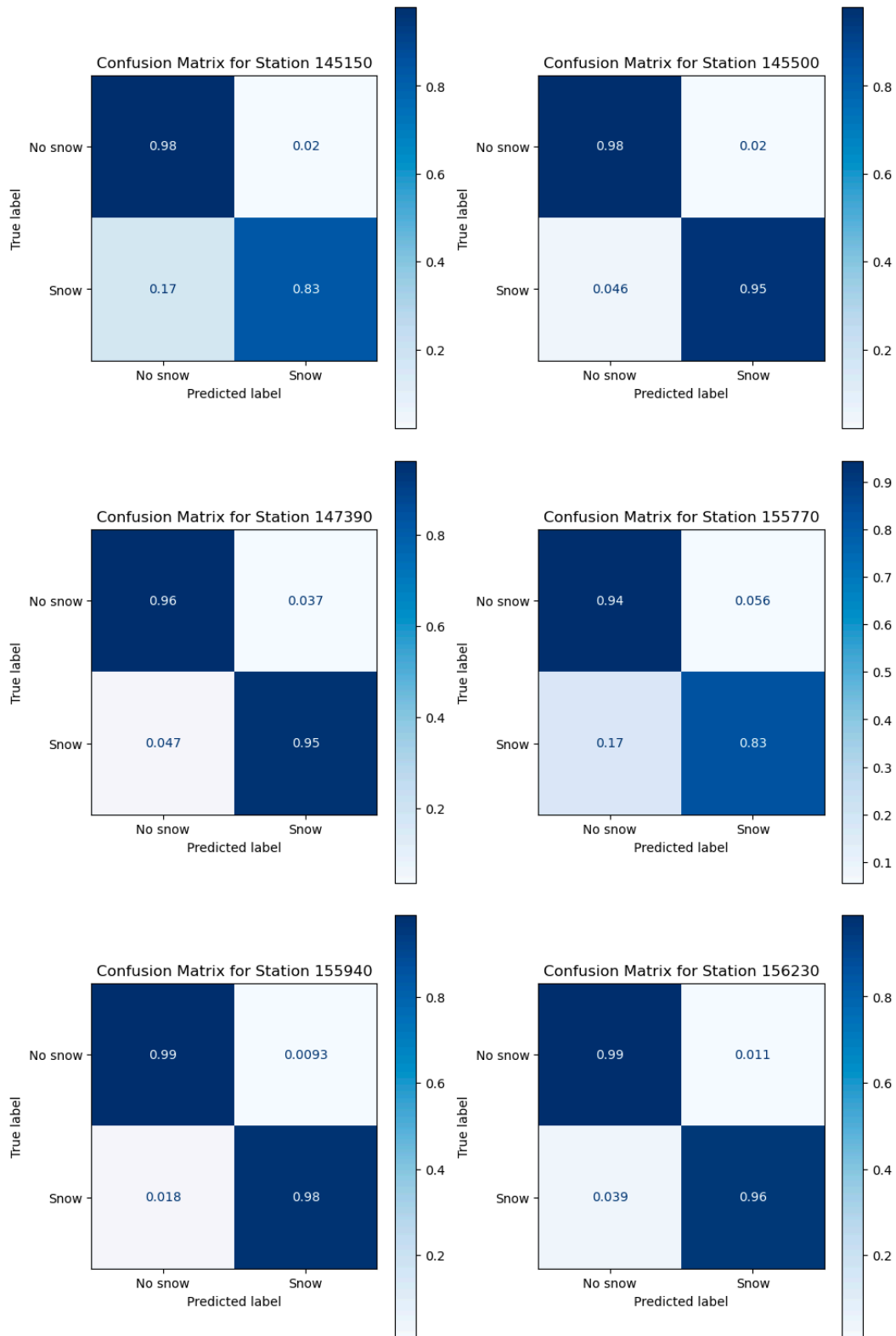


Figure 24: Confusion matrix of Sentinel-2 FSCOG snow product for individual stations evaluated on SMHI ground truth data. Values normalized by number of acquisitions per snow product.

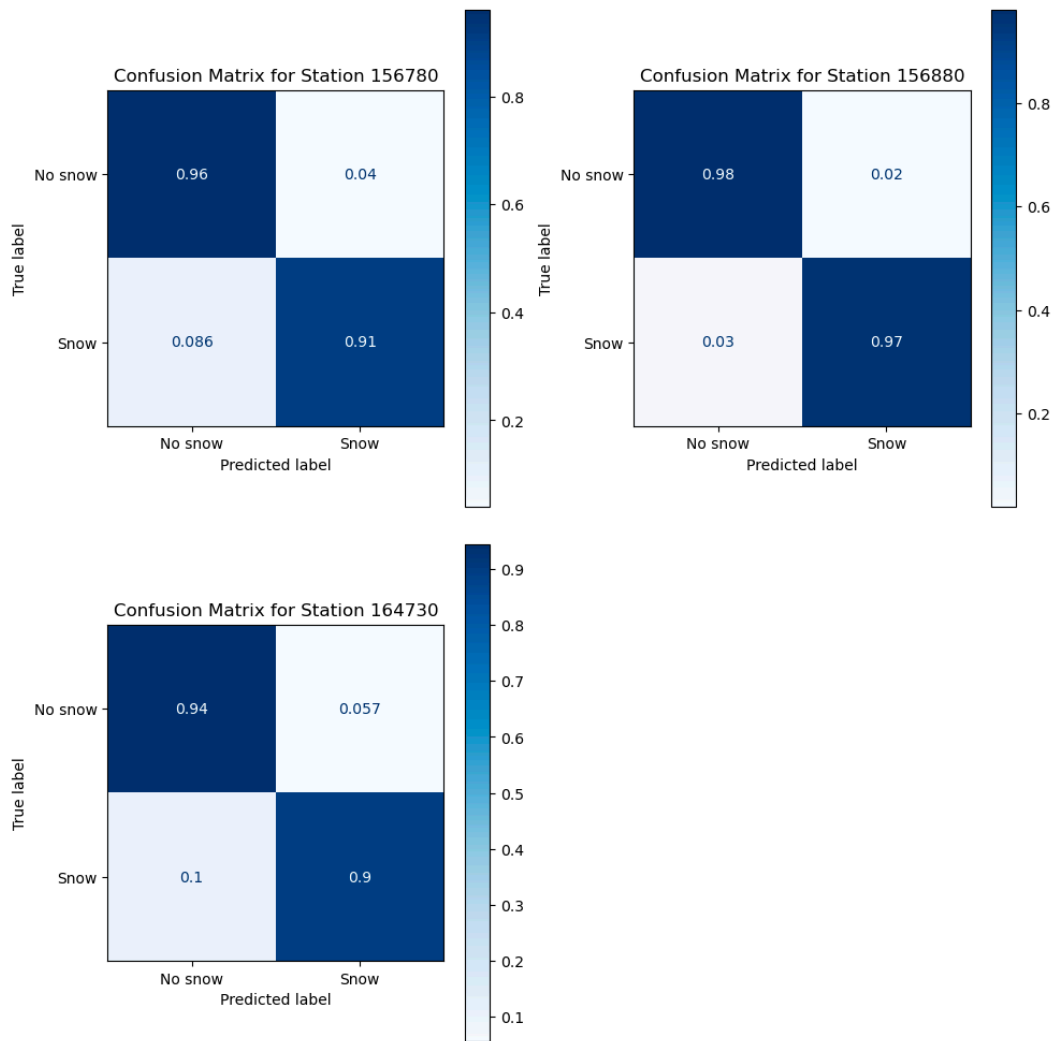


Figure 25: Confusion matrix of Sentinel-2 FSC<sub>OG</sub> snow product for individual stations evaluated on SMHI ground truth data. Values normalized by number of acquisitions per snow product.

## 9.1.2 IMS

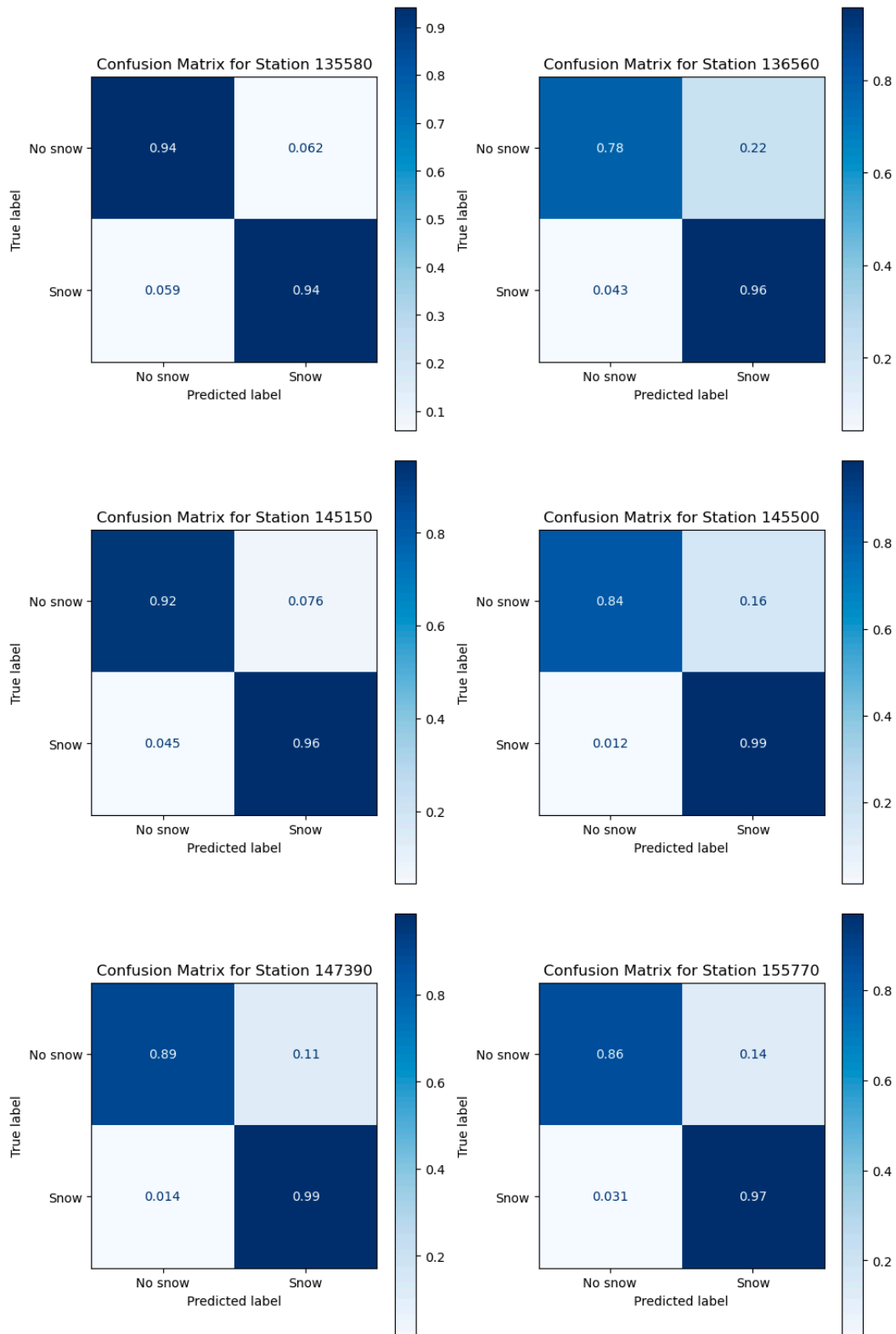


Figure 26: Confusion matrix of IMS snow product for individual stations evaluated on SMHI ground truth data. Values normalized by number of acquisitions per snow product.

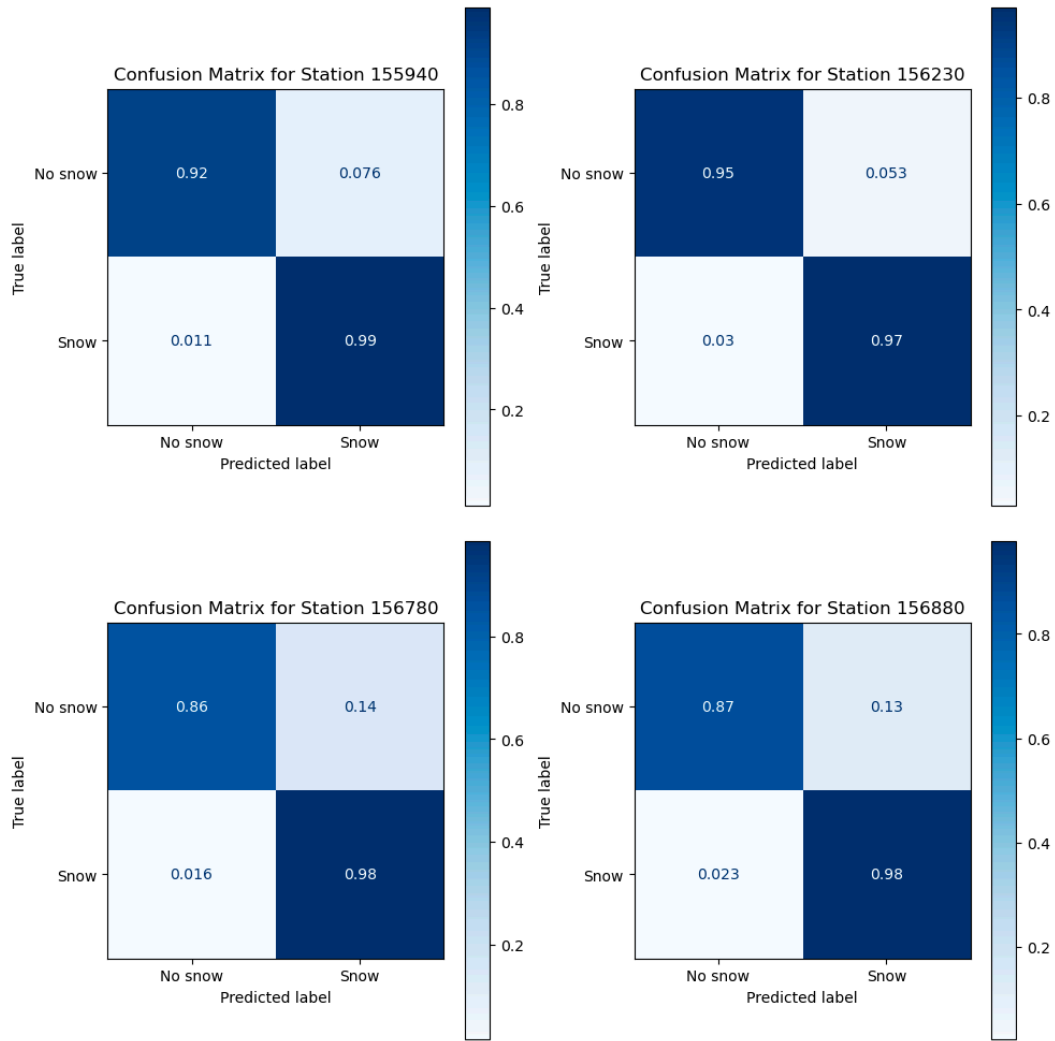


Figure 27: Confusion matrix of IMS snow product for individual stations evaluated on SMHI ground truth data. Values normalized by number of acquisitions per snow product.

### 9.1.3 V2

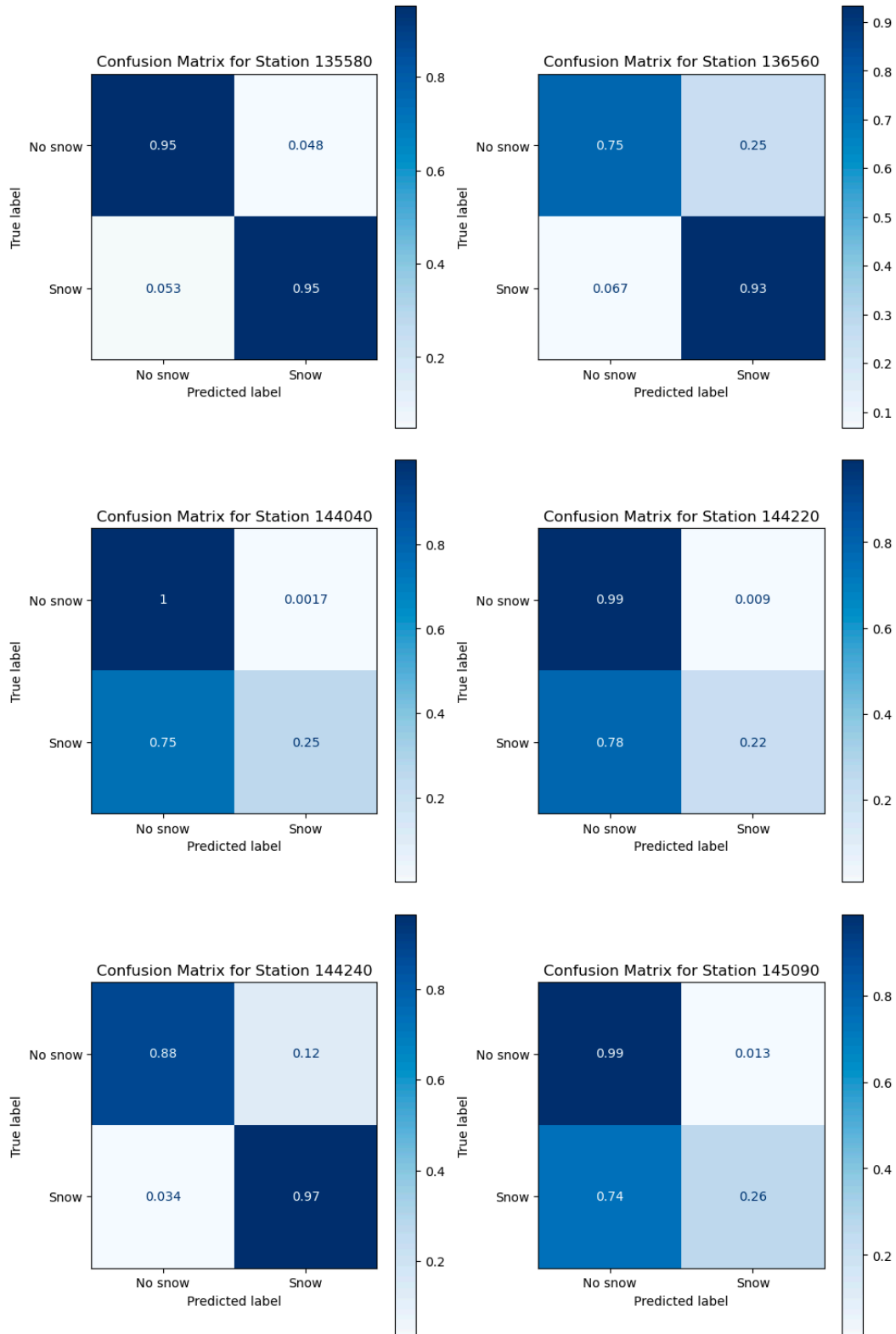


Figure 28: Confusion matrix of V2 snow product for individual stations evaluated against SMHI ground truth data. Values normalized by number of acquisitions per snow product.

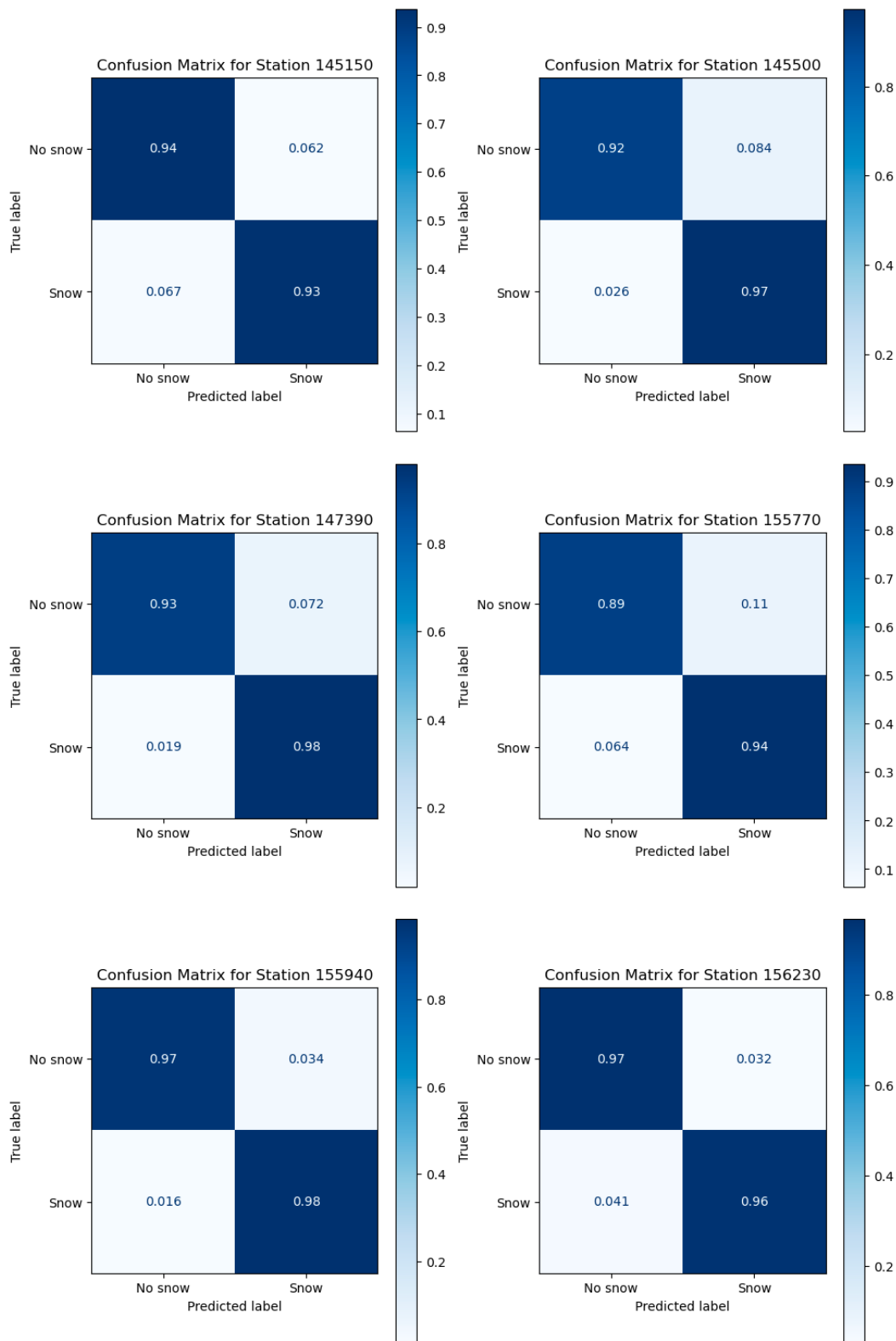


Figure 29: Confusion matrix of V2 snow product for individual stations evaluated on SMHI ground truth data. Values normalized by number of acquisitions per snow product.

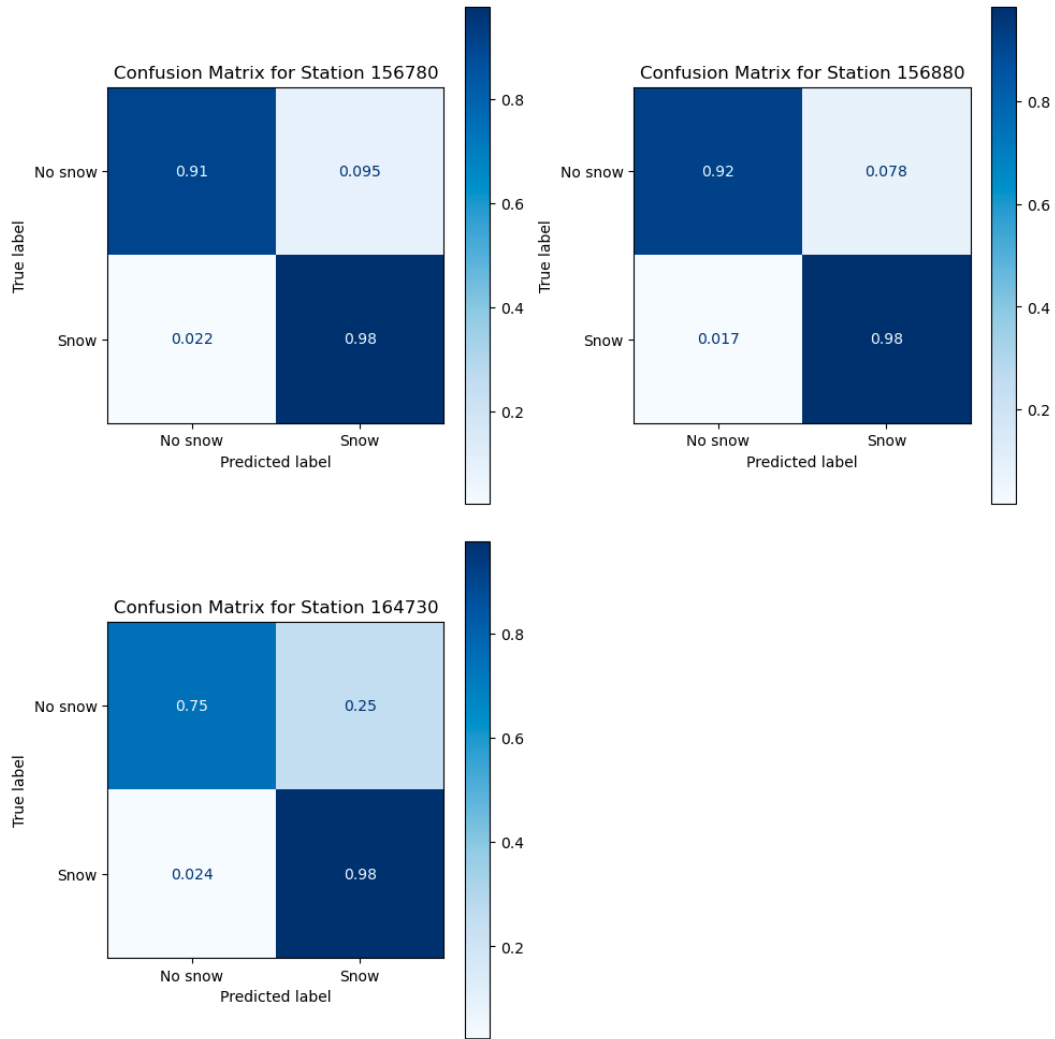


Figure 30: Confusion matrix of V2 snow product for individual stations evaluated on SMHI ground truth data. Values normalized by number of acquisitions per snow product.